The following document is a pre-print version of:

Delpit S, Ross P-S, Hearn BC (2014) Deep-bedded ultramafic diatremes in Missouri River Breaks volcanic field, Montana, USA: 1 km of syn-eruptive subsidence. Bull. Volc. 76:Art. 832

Deep bedded ultramafic diatremes in the Missouri River Breaks volcanic field, Montana, USA: 1 km of syn-eruptive subsidence

Séverine Delpit[1,*], Pierre-Simon Ross[1] and B. Carter Hearn Jr[2]

[1]Institut national de la recherche scientifique,
490 rue de la Couronne, Québec (Qc) G1K 9A9, Canada
[2]United States Geological Survey, 954 National Center, Reston VA 20192, USA
[*]Corresponding author, severine.delpit@gmail.com

Abstract

The ultramafic Eocene Missouri River Breaks volcanic field (MRBVF, Montana, United States) includes over 50 diatremes emplaced in a mostly soft substrate. The current erosion level is 1.3-1.5 km below the pre-eruptive surface, exposing the deep part of the diatreme structures and some dikes. Five representative diatremes are described here; they are 200-375 m across and have sub-vertical walls. Their infill consists mostly of 55-90% bedded pyroclastic rocks (fine tuffs to coarse lapilli tuffs) with concave-upward bedding, and 45-10% non-bedded pyroclastic rocks (medium lapilli tuffs to tuff breccias). The latter zones form steep columns 15-135 m in horizontal dimension, which cross-cut the bedded pyroclastic rocks. Megablocks of the host sedimentary formations are also present in the diatremes, some being found 1 km or more below their sources. The diatreme infill contains abundant lithic clasts and ash-sized particles, indicating efficient fragmentation of magma and country rocks. The spherical to sub-spherical juvenile clasts are non-vesicular. They are accompanied by minor accretionary lapilli and armored lapilli. The deposits of dilute pyroclastic density currents are locally observed.

Our main interpretations are as follows: (1) the observations strongly support phreatomagmatic explosions as the energy source for fragmentation and diatreme excavation; (2) the bedded pyroclastic rocks were deposited on the crater floor, and subsided by 1.0-1.3 km to their current location, with subsidence taking place mostly during the eruption; (3) the observed non-bedded pyroclastic columns were created by debris jets that punched through the bedded pyroclastic material; the debris jets did not empty the mature diatreme, occupying only a fraction of its width, and some debris jets probably did not reach the crater floor; (4) the mature diatreme was nearly always filled and buttressed by pyroclastic debris at depth – there was never a 1.3-1.5 km-deep empty hole with sub-vertical walls, otherwise the soft substrate would have collapsed inward, which it only did near the surface, to create the megablocks. We infer that syn-eruptive subsidence shifted down bedded pyroclastic material and shallow sedimentary megablocks by 0.8-1.1 km or more, after which limited post-eruptive subsidence occurred. This makes the MRBVF diatremes an extreme end-member case of syn-eruptive subsidence in the spectrum of possibilities for maar-diatreme volcanoes worldwide.

Keywords: diatreme, Missouri River Breaks, ultramafic, phreatomagmatism, subsidence, maar

1. Introduction

Maar-diatreme volcanoes consist of a maar crater, the surrounding tephra ring, and the underlying diatreme and dikes (see review by White and Ross 2011 and references therein). A number of field studies describe maars and tephra rings (e.g., Buchel and Lorenz 1993; Aranda-Gómez and Luhr 1996; Németh et al. 2001; Vasquez and Ort 2006; Auer et al. 2007; Carrasco-Núñez et al. 2007; Befus et al. 2008; Ort and Carrasco-Núñez 2009; Sottili et al. 2009; Ngwa et al. 2010; Alvarado et al. 2011; Ross et al. 2011; Valentine 2012; Jordan et al. 2013), but few non-kimberlitic diatremes, root zones and underlying dikes have been documented in detail (e.g., Hearn 1968; Lorenz 1986; White 1991; White and McClintock 2001; Hooten and Ort 2002; McClintock and White 2006; Ross and White

2006; Kwon and Sohn 2008; Calvari and Tanner 2011; Lefebvre et al. 2013). Therefore, volcanic processes occurring in diatremes remain poorly understood, especially since they have not been observed during historical maar eruptions (e.g., Kienle et al. 1980; Self et al. 1980) given their underground nature.

By combining reviews of historical maar eruptive activity (e.g., White and Ross 2011), laboratory experiments on explosive and non-explosive magma-water interaction (e.g., Zimanowski et al. 1997; Kurszlaukis et al. 1998; Schipper et al. 2011) and debris jets (Ross et al. 2008a, 2008b), documentation of maar tephra ring characteristics (see above), and, importantly, studies of partly eroded diatremes (see above), a consistent general model has emerged for the internal workings of diatremes (White and Ross 2011; Valentine and White 2012). Large-scale analogue experiments are also being added to the dataset on maar-diatreme volcanoes (Valentine et al. 2012; Ross et al. 2013; Taddeucci et al. 2013). However, many questions remain, for example, it is not clear why magma-aquifer interactions are sometimes explosive, and sometimes not. Only a small number of well-exposed diatremes have been described in detail in the literature, and the full range of deposits and, probably, eruptive processes is not known.

White and Ross (2011) emphasize the variability of deposits in the upper part of diatremes, ranging from bedded to non-bedded. Diatreme emplacement models will of course be strongly influenced by the type of deposits present. Within the bedded deposits, two types are distinguished by White and Ross (2011): "one forms during diatreme excavation and subsides as the eruption progresses (type I); the other develops late in an eruption, subsequent to major excavation, and hence is not deeply subsided, commonly filling the syn-eruptive crater and grading upward into surficial tuff or scoria cones (type II)". Diatremes from the Eocene Missouri River Breaks volcanic field (MRBVF) in Montana, USA (Hearn 1968) are presented by White and Ross (2011) as the type example of the type I bedded pyroclastic infill with extensive subsidence, but these diatremes have not been described in detail.

In this paper, we document five representative MRBVF diatremes using field mapping, rock slabs and petrography. The diatreme infills are mostly bedded at current erosion levels, which are 1.3-1.5 km below the pre-eruptive surface (Hearn 2012). The presence of bedded pyroclastic deposits at these depths cannot be explained without a significant amount of syn-eruptive subsidence, which we calculate as 0.8-1.1 km or more. In contrast, in other volcanic fields, the deep infill of diatremes is typically non-bedded (Hawthorne 1975; Lorenz 2003; Cas et al. 2008a; White and Ross 2011; Gernon et al. 2012) and syn-eruptive subsidence on this scale is rarely reported (Lorenz 1973, 1975, 1986, 2000, 2007; Lorenz and Kurszlaukis 2007).

2. Geological setting

The MRBVF is located in north-central Montana, about 160 km east of Great Falls and 200 km north of Billings (Fig. 1). This Paleogene volcanic field consists exclusively of partially eroded diatremes and ultramafic dikes; all surface manifestations of volcanism have been removed by erosion.

The MRBVF is part of the Paleogene Great Plains alkalic province that spans South Dakota, Montana, Wyoming and southern Alberta (Duke 2009; Fig. 1); in Montana, this province is known as the Montana alkalic province (Dudàs 1991; O'Brien et al. 1991, 1995; MacDonald et al. 1992; Christiansen et al. 2002; Dostal et al. 2003; Mirnejad and Bell 2006). During the Late Cretaceous epoch, extrusive and intrusive magmatic activity occurred in Montana and the surrounding areas, fueled by an asthenospheric window formed by the subduction of the mid-ocean ridge separating the Kula plate, to the north, and the Farallon plate, to the south, beneath the North-American plate (Duke 2009).

2.1 Pre-MRBVF rocks

The deep basement beneath the Montana alkalic province consists of Archean and Proterozoic rocks. The MRBVF is located in the Precambrian Great Falls tectonic zone, which separates the Wyoming Archean Province to the southeast from the Medicine Hat block to the northwest (Irving and Hearn 2003). In the study area, this Precambrian basement is covered by about 1 km of Paleozoic to Jurassic sedimentary rocks and by another kilometer of Cretaceous sedimentary rocks (Hearn 1968). The MRBVF diatremes were emplaced in predominantly Upper Cretaceous to lower Eocene sedimentary formations principally consisting of sandstones and shales (Figs. 2 and 3). These formations remain mostly unconsolidated to poorly consolidated today, although some sandstone and siltstone beds are well cemented. The sedimentary sequence has been well studied (Swenson 1955; Miller and Appel 1997; Porter and Wilde 2001; Wilde and Porter 2001) and large clasts or megablocks in the diatremes can typically be assigned confidently to a source formation (e.g., Hearn 1968). The sedimentary sequence is part of the Northern Great Plains aquifer system; the major aquifers are the Tertiary and Cretaceous sandstones as well as the Paleozoic carbonaceous rocks, notably in the Williston and Powder River basins (Downey and Dinwiddie 1988; Miller and Appel 1997). Within the stratigraphic section shown in Figure 3, many of the formations are known aquifers except the Upper Cretaceous Bearpaw Shale, Claggett Shale, and shale members of the Colorado Group. The abundance of water in these sediments today indicates that the rocks

would have had the properties necessary to serve as aquifers during the early Eocene, at the time of volcanism, when the climate was warmer and wetter (Bowen et al. 2004; Foreman et al. 2012).

2.2 The Missouri River Breaks volcanic field

Nearly 50 diatremes and more than a dozen dykes, emplaced between 49 and 47 Ma (conventional K/Ar), are reported in the MRBVF along a 080° trend, over a length of 140 km (Hearn 1968, 2012; Irving and Hearn 2003). Ultramafic magmas in the MRBVF include monticellite melnoite, alnöite, aillikite, kimberlite and carbonatite (Irving and Hearn 2003); melnoite is dominant (Hearn 2012). Petrologic details will be presented elsewhere. The diatremes are 50 to 520 m in maximum dimension in plan view, with circular to elliptical shapes (Hearn 2012). The current level of exposure is 1.3-1.5 km below the pre-eruptive surface based on measurements of sedimentary strata in the Bearpaw Mountains, 15 to 45 km north of the study area (Hearn 1964). At this level of exposure, the pyroclastic fill of the diatremes is mostly bedded, with centimetric to metric beds defining concave-upward shaped structures ("centroclinal bedding"; Francis 1970); zones of non-bedded pyroclastic rocks with near-vertical contacts, and minor ultramafic dikes, are also present (Hearn 1968). Ring faults surround the diatremes (Hearn 1968; Fig. 3) and are marked by "slickenside surfaces with or without tectonic breccia" (Hearn 1979). Sedimentary megablocks with steep dips, called "downfaulted slices" by Hearn (1968), occur in the marginal areas of the diatremes and reach 180 m in long dimension; these are mostly derived from the shallow formations (Fig. 3). Little volcanological information has been published on the MRBVF diatremes since the 1960s.

3. Methods

For the current study, four representative diatremes (Black Butte, Ervin Ridge, Hay Coulee and Lone Tree Ridge) were examined and sampled in detail over six weeks during summer 2009 (Delpit 2013; Figs. 4-7), out of the more than 50 diatremes mapped by the third author in the 1960's and the 1970's (partial compilation in Hearn 2009). The Bullwhacker Coulee diatreme is also used as a representative example here (Fig. 8), although it was not sampled by Delpit (2013) since its outcrops are very steep. These five diatremes are all located in the badlands area north of the Missouri River (Fig. 2) and their main characteristics and locations are listed in Table 1. Some 150 new samples were collected and 61 were thin sectioned (Delpit 2013).

For each of the four diatremes studied in detail, estimates of clast shape, grain size and components (in the field and on slabs in the lab) of the pyroclastic material were visually assessed; stratigraphic logs were compiled for the bedded rocks where possible. The volcanic micro-textures are partly obscured by alteration and most of the primary minerals have been replaced by secondary ones: this precluded petrographic clast counts or grain-size determinations.

4. Field observations

The immediate host rocks for the five diatremes at the current levels of exposure are the Judith River Formation (soft sandstones and siltstones) and the Bearpaw Shale (soft shales). At Bullwhacker Coulee, steep exposures show that the Judith River Formation layers are bent downward near the diatreme (Fig. 9a). It is likely that the same phenomenon occurs elsewhere because partial "collars" of downward-displaced sedimentary rocks are found around every studied/visited diatreme (Figs. 4 to 8); displacement distances are on the order of hundreds of meters.

At the current level of exposure, the studied diatremes range in horizontal diameter from 200 to 375 m (Table 1) with very steep walls (up to 90°). In map view, they have mostly circular to elliptical outlines. The dominant infilling material consists of bedded pyroclastic rocks (section 4.1), with lesser proportions of non-bedded pyroclastic rocks (section 4.2).

Megablocks of sedimentary formations, derived from higher levels in the sequence, are also found in the diatremes, commonly near their margins (Fig. 3). Typically the long axes of the megablocks are sub-vertical. For example, at Bullwhacker Coulee diatreme, a Wasatch Formation megablock 35 m long in plan view and 30 m high is present at the level of the Judith River Formation (Fig. 9a), at least 1.1 km below its original position.

Coherent ultramafic dykes 10-30 cm-wide occur within and just outside diatremes, some of them in partial "ring-fault" positions (e.g., Figs. 5, 7 and 8). These coherent rocks are non-vesicular and contain euhedral to subhedral olivine phenocrysts and/or micro-phenocrysts in a microcrystalline groundmass. Some dykes contain up to 5% sedimentary fragments up to 5 cm across, and some contain up to 5% spherical to sub-spherical juvenile pyroclasts up to 1 cm across. These clasts are randomly distributed in the rock. The diatremes also contain late coherent and non-vesicular ultramafic plugs a few meters in diameter (e.g., Figs. 4 to 8) with similar petrographic characteristics to the coherent ultramafic dikes. In Black Butte, Hay Coulee and Ervin ridge diatremes, the infill is cut by 1-30 cm-thick beige sandstone and black shale clastic dykes (Delpit 2013).

4.1. Bedded pyroclastic rocks

The studied diatreme structures are mostly filled with bedded pyroclastic rocks (Figs. 4-8, 9a, b). Inward dips of the beds are very steep along the diatreme

margins, up to 70° in the Lone Tree Ridge diatreme (Figs. 4-8, 9c), and become near horizontal toward the diatreme center as in Bullwhacker Coulee diatreme (Fig. 9a). In the Lone Tree Ridge diatreme and elsewhere, unconformities are present in the bedded sequence (but no paleosoils or other evidence of long eruptive pauses). Most beds appear massive internally. Locally, we also identified low-angle cross-bedding within pyroclastic rocks (e.g., Fig. 9c).

Several representative stratigraphic sections ranging in height from 2.7 to 22.7 m were logged in Black Butte, Lone Tree Ridge and Hay Coulee diatremes to characterize the bedded pyroclastic rocks (e.g., Fig. 10). In all sections combined, the thickness of the pyroclastic beds ranges from three centimeters to ten meters and the grain size varies from fine tuff to coarse lapilli tuff (classification of White and Houghton 2006; Table 2). The rarer tuff beds are beige and consolidated whereas the dominant lapilli tuff beds are greenish, consolidated and some, with low amounts of fine ash, are easily broken with one's fingers.

4.2. Non-bedded pyroclastic rocks

Zones of non-bedded pyroclastic material also occur in the five diatremes, but are proportionately minor relative to the bedded pyroclastic rocks (Figs. 4 to 8). These zones occupy 15-45% of the exposures (Table 1) and are identified as columns that cut across the bedded pyroclastic rocks. Contacts between bedded and non-bedded pyroclastic units are sharp and steep where clearly observed (e.g., Fig. 11). In plan view, the non-bedded zones have mostly irregular shapes with dimensions ranging from 15x30 m to 135x45 m and occur throughout the diatreme. Generally, these non-bedded deposits are medium to coarse lapilli tuffs and tuff breccias. The pyroclastic material is on average coarser than in the bedded pyroclastic material because it contains sedimentary blocks and less ash (section 4.3). Within single diatremes, different non-bedded zones tend to have different grain sizes and components, as indicated in the map legends.

4.3 Components and proportions

The bedded and non-bedded pyroclastic infill of each diatreme is composed of variable proportions of (i) juvenile blocks/bombs and lapilli; (ii) lithic blocks and lapilli; and (iii) the undifferentiated ash fraction (Fig. 12).

The juvenile fraction is predominantly composed of ultramafic spherical to sub-spherical pyroclasts (Fig. 13a), of free altered olivine crystals up to 1 cm across, and, in smaller amounts, of ash aggregates. The spherical to sub-spherical juvenile pyroclasts are composed of a non-vesicular and finely crystalline ultramafic material, with or without cores. Detailed study of 227 juvenile lapilli revealed that 67% have a central or eccentric core (lithic clast or altered olivine crystal), coated by ultramafic juvenile material, whereas the other 33% lack cores. Spherical to sub-spherical juvenile pyroclasts will be further described and interpreted in a separate publication.

Two types of ash aggregates occur. The first one is armoured lapilli, with each lapillus composed of unconsolidated beige fine ash surrounding an altered olivine crystal (Fig. 13b). Schumacher and Schmincke (1991) define an armoured lapillus as "a lapilli-sized rock fragment that is coated in ash" with the volume of the enclosed particle larger than that of the surrounding agglomerated ash. If the volume of the enclosed particle is comparatively smaller, then the term "accretionary lapillus" applies. Armoured lapilli are found locally in the bedded pyroclastic rocks of Black Butte and Hay Coulee diatremes. The second type of ash aggregate lacks a central core and has been observed in both bedded and non-bedded pyroclastic rocks from each diatreme. These ones are also of lapilli size (<1 cm to 3.5 cm across) are spherical to sub-spherical (Fig. 13c) or angular (not shown). They are composed of unconsolidated to semi-consolidated beige fine ash with free altered olivine crystals. This second type of ash aggregate may represent accretionary lapilli (for the spherical clasts) or recycled tuff fragments (for the angular ones).

The lithic material in the diatreme infill is mostly from the lower Eocene Wasatch Formation and the Paleocene Fort Union Formation (Fig. 3) and is composed of sub-angular to sub-rounded rock fragments, and quartz and feldspar grains. Abundant pebbles and boulders derived from the Wasatch Formation are also identified in the pyroclastic deposits.

Within individual stratigraphic logs of bedded pyroclastic rocks, the proportion of juvenile fragments, lithic fragments, and undifferentiated ash is very variable. In section HC-042 for example, the juvenile fraction varies from 2% to 48% (average of 24%; stdev of 15%); the lithic fraction varies from 2% to 22% (average of 10%; stdev of 7%) and the ash fraction represents between 36% and 96% of individual beds (Table 2). For all sections combined, the juvenile fraction varies from 4% to 54%; the lithic fraction varies from 2% to 40% and the ash fraction represents between 5% and 80% of individual beds (Table 2).

The non-bedded pyroclastic material, based on a total of 13 stations (four at Hay Coulee; two at Black Butte; four at Lone Tree Ridge and three at Ervin Ridge), contains 0%-28% altered olivine crystals (average 11%; stdev 11%); 13%-60% spherical to sub-spherical juvenile pyroclasts (average 34%; stdev 16%); 15%-65% lithic fragments (average 39%; stdev 16%). The ash fraction varies from 6% to 32% (average 16%; stdev 9%). It is noteworthy that the non-bedded material generally contains much less ash (average

16%) than do the bedded pyroclastic rocks (average 45%).

5. Discussion

This discussion first establishes that explosive magma-aquifer interactions are responsible for creating the MRBVF diatremes. That allows us to interpret our field observations within the general phreatomagmatic maar-diatreme framework (e.g., Lorenz 1986; White and Ross 2011; White and Valentine 2012). Specifically we focus this discussion on the influence of the substrate on the morphology of these diatremes, and on the role of syn-eruptive subsidence during the eruptions. A MRBVF-specific diatreme emplacement model is then proposed, integrating all our observations and interpretations. Finally, we compare the MRBVF diatremes with class 1 kimberlitic diatremes, since they have many features in common, despite strikingly different models having been proposed for their origin.

5.1 Phreatomagmatic origin

We propose that phreatomagmatic activity is responsible for generating the MRBVF diatremes and overlying maars (now eroded away). The first line of evidence for a phreatomagmatic origin is the high proportion of lithic fragments in the diatreme rocks. In the combined lapilli and blocks/bombs fractions, the average proportions of lithic fragments are 45% and 39% for bedded and non-bedded pyroclastic rocks, respectively. Lithic fragments reach 72% in some bedded rocks and 65% in some non-bedded rocks. Such high lithic contents are typical of phreatomagmatic deposits, especially those of maar-diatreme volcanoes (e.g., Lorenz 1973, 1975, 1985, 1986; Wohletz and Sheridan 1983; Fisher and Schmincke 1984; Cas and Wright 1987; Zimanowski 1998; Lorenz et al. 2002; McClintock and White 2006; Befus et al. 2008; White and Ross 2011; Son et al. 2012). In contrast, the magmatic equivalent to maar-diatremes volcanoes, the scoria cones (Lorenz 2000), typically have very low lithic contents (<1%) (Vespermann and Schmincke 2000; Bertotto et al. 2006; Pioli et al. 2008; Valentine 2012). More powerful magmatic eruptions, such as vulcanian and subplinian to plinian eruptions, have deposits that can be richer in lithic fragments than those of scoria cones due to the clearing of the vent during the eruption (Cioni et al. 2000; Morrissey and Mastin 2000). However, the eruption rates and erupted volumes for sub-plinian to plinian eruptions are orders of magnitude higher than those of maar-diatreme or scoria cone eruptions (Valentine and White 2012), making comparisons difficult. The majority of the identifiable lithic fragments in the MRBVF diatremes are derived from the shallow and unconsolidated lower Eocene Wasatch Formation and Paleocene Fort Union Formation, i.e. from the top of the stratigraphic sequence (Fig. 3). The reasons for the dominance of shallow lithic fragments in diatremes and maars have been discussed by Valentine (2012), Valentine and White (2012), Lefebvre et al. (2013) and references therein.

The second line of evidence for the phreatomagmatic origin of the MRBVF diatremes is the abundant ash in the pyroclastic rocks, which indicates efficient fragmentation (Büttner and Zimanowski 1998; Zimanowski 1998; Büttner et al. 1999, 2006; Zimanowski et al. 2003; Raue 2004). The bedded pyroclastic rocks contain more ash-sized particles on average (45%) than the non-bedded pyroclastic rocks (16%). We think this is a primary feature and reflects emplacement processes of the bedded vs. non-bedded deposits, as explained in section 5.3.

The third line of evidence for a phreatomagmatic origin is the absence of vesicles in juvenile fragments and coherent dykes in the MRBVF diatremes. Except for the largest juvenile fragments, phreatomagmatic fragmentation preserves the bubbles as present in the magma at the time of fragmentation; many studies of phreatomagmatic juvenile clasts show a low vesicularity, possibly because vesiculation was arrested early (Houghton and Wilson 1989; Ross and White 2006, 2012; Auer et al. 2007; Downes et al. 2007; McClintock et al. 2009; Pardo et al. 2009; Sottili et al. 2012) or from degassing prior to fragmentation. In contrast, magmatic fragmentation of mafic to ultramafic magma typically produces scoria or spatter (Cashman et al. 2000; Vergniolle and Mangan 2000; Vesperman and Schmincke 2000; Lautze and Houghton 2007; Brown et al. 2012a). The abundance of ash-sized particles in the rocks combined with the absence of vesicles in juvenile clasts shows efficient magma fragmentation without the influence of magmatic volatiles.

The fourth evidence for a phreatomagmatic origin is the presence of armoured lapilli and accretionary lapilli in the MRBVF diatremes. These are most often, but not exclusively, observed in phreatomagmatic deposits, and form because of moisture in the eruptive column (Waters and Fisher 1971; Fisher and Schmincke 1984; Schumacher and Schmincke 1991, 1995; White 1991; Gilbert and Lane 1994; Auer et al. 2007; Carrasco-Núñez et al. 2007; Németh et al. 2008; Sottili et al. 2009, 2012; Brown et al. 2012a; Van Eaton and Wilson 2013).

The fifth evidence is the presence of low-angle cross bedding in the pyroclastic rocks. Given the context, we interpret such structures as formed by dilute pyroclastic density currents. Such currents are typical of phreatomagmatic eruptions, including in maar tephra rings (Moore et al. 1966; Moore 1967; Fisher and Waters 1970; Waters and Fisher 1971; Crowe and Fisher 1973; Lorenz 1973, 2003; Chough and Sohn 1990; White 1991; Aranda-Gómez and Luhr 1996;

Freda et al. 2006; Gençalioglu-Kuscu et al. 2007; Valentine 2012; Valentine et al. 2012).

Finally it is worth noting that aquifers currently occupy most of the sedimentary formations in which the MRBVF diatremes were emplaced, suggesting that, given the climate at the time, groundwater would also have been present here in early Eocene time. In contrast with the several indicators of phreatomagmatism just listed, we find no specific evidence for magmatic fragmentation in the MRBFV diatremes.

5.2 Origin of pyroclastic beds, multiple explosions and recycling

In some other diatremes, bedding is attributed at least in part to eruptions from nearby vents (e.g., Gernon et al. 2013). But for the MRBVF diatremes, Hearn (1968) notes that the coarseness of the pyroclastic rocks and the wide separation between diatremes indicates that "each diatreme was filled by its own eruptions".

The mode of deposition of each pyroclastic bed cannot be established with confidence given the internally structureless appearance of most beds and their state of alteration, but we infer that each bed was deposited on the crater floor by fallback, fallout or pyroclastic density currents. Collapse of the tephra ring into the crater would also have contributed pyroclastic material.

Bedding thickness is a few centimeters to a few meters (Table 2), meaning that if this style of bedding continued to the (now eroded) crater floor, there were several thousand beds filling each diatreme at the end of the eruptions. The layers have a range of thicknesses and grain sizes, and indicate that numerous explosions of various intensities, and possibly locations, occurred in the diatremes. Multiple explosions are typical of maar-diatreme volcanoes (e.g., Lorenz, 1975; White and Ross 2011 and references therein).

The unconformities observed in the sequence have two possible interpretations. They may be the result of a sudden change in the location of the eruptive site laterally on the crater floor. The new pyroclastic deposits would then cut and overlie the previous ones. Another possibility is that bedded pyroclastic deposits from the tephra ring slumped into the crater.

Angular ash-aggregate clasts are inferred to represent fragments of tuff beds that were recycled by later eruptions, in the same way that juvenile fragments can be recycled (Houghton and Smith 1993; Houghton et al. 1999; Ross and White 2012). These tuff beds may have slumped from the tephra ring or have been initially deposited on the crater floor.

5.3 Non-bedded pyroclastic zones and debris jets

Columns of non-bedded pyroclastic material cut across the bedded pyroclastic rocks. Such columns have also been observed in other volcanic systems (White 1991; Naidoo et al. 2004; Nowicki et al. 2004; Stiefenhofer and Farrow 2004; McClintock and White 2006; Ross and White 2006; Lefebvre et al. 2013). They are commonly found in the typically non-bedded lower parts of diatremes (White and Ross 2011; Lefebvre et al. 2013). The columns are inferred to result from the passage of debris jets through the diatreme-filling material (McClintock and White 2006; Ross and White 2006; Ross et al. 2008a, 2008b; White and Ross 2011). Debris jets are "upward-moving streams of volcaniclastic debris, steam, magmatic gases +/- liquid water droplets" that form after phreatomagmatic explosions in diatremes (Ross and White 2006). In the MRBVF diatremes, these non-bedded pyroclastic rocks are similar in terms of components but coarser on average than bedded pyroclastic rocks. They have large amounts of sedimentary blocks and in some cases coarser (up to 15 cm) spherical to sub-spherical juvenile pyroclasts, and less ash-sized particles. Our preferred hypothesis for this grain size difference is that the debris jets that generated the preserved columns (at the current exposure level) were formed by less powerful explosions with less efficient fragmentation than others, possibly shallower, that fed eruptive plumes in the atmosphere. In other words, the explosions that created the non-bedded columns did not necessarily send material all the way up to the crater floor, whereas the explosions that *did* vent were more intense (or shallower) and left fewer non-bedded deposits in the diatreme. This explains in part the grain-size difference observed between bedded pyroclastic rocks in the diatreme (and the beds in the inferred tephra ring) vs. the coarser non-bedded rocks in the diatreme.

5.4 Role of the unconsolidated substrate

The nature of the substrate of maar-diatreme volcanoes ("hard" vs. "soft") has been proposed to influence their forms (e.g., Lorenz 2003; Auer et al. 2007; Németh and Martin 2007; Németh et al. 2010). Specifically, it is often proposed that soft substrates produce broad bowl-shaped craters and narrow (and perhaps shallow) diatremes, whereas maars in hard substrates can have sub-vertical walls with deep, conical diatremes (Lorenz 2003; Field et al. 2008; Martin-Serrano et al. 2009). However, the larger diameter/depth ratios of craters in soft substrates may largely be due to post-eruptive modifications (Ross et al. 2011) and the diatremes may actually be very similar in both types of substrates (White and Ross 2011). An illustration of the latter point is the MRBVF diatremes, which were emplaced in a predominantly unconsolidated to poorly consolidated substrate. The exposed parts of the diatremes are situated 1.3 to 1.5 km below the pre-eruptive surface and, at these depths, diatreme walls are nearly vertical and the

diameters are several hundred meters across, just as would be expected for deep diatremes emplaced in a hard substrate. The shape of the MRBVF diatremes does not appear to have been affected by the predominantly soft nature of the rocks in which they were emplaced. If there had been a deep (>1 km) open hole with nearly vertical walls, in soft sedimentary strata, the walls would have collapsed, as also noted by Hearn (1968) and Lorenz and Kurszlaukis (2007). But the walls did not collapse at the current exposure levels, because the diatremes were nearly always filled and buttressed by pyroclastic debris at these depths.

A question may arise about the sedimentary material originally present in the deep part of what is now a diatreme: if there was never a deep open hole (an "empty diatreme"), how was this deep lithic fraction expulsed? Some of it is still present as clasts in the diatreme fill, whereas other lithic fragments travelled inside debris jets towards, or to, the crater floor. These debris jets did not occupy the full width of the diatreme, as they would then have destroyed all bedding.

5.5 Syn-eruptive subsidence

Subsidence can play an important role both during and after the eruption of maar-diatreme volcanoes (Lorenz 1973, 1975, 1986, 2003, 2007; McCallum 1976; Pirrung et al. 2001; Suhr et al. 2006; Németh et al. 2007; Brown et al. 2008; Geshi et al. 2011; White and Ross 2011). Evidence for subsidence in the MRBVF diatremes includes: (i) concave-upward bedding of pyroclastic rocks; (ii) collars of downward-displaced sedimentary formations surrounding the diatremes, as well as the downward curvature (drag folds) of the country rock layers near the diatreme walls; and (iii) the presence of megablocks that in some cases have travelled downward more than 1 km inside the diatremes. Assuming, conservatively, that the crater was 200 m to 300 m deep at the end of the eruption (based on the deepest maars known, see Suhr et al. 2006, Ross et al. 2011), and that the pyroclastic beds were deposited on the crater floor but are currently exposed 1.3-1.5 km below the pre-eruptive surface (Hearn 2012), the total amount of subsidence needed at the MRBVF diatremes is 1.0-1.3 km, or more if the crater was shallower..This figure combines syn-eruptive and post-eruptive subsidence. Hearn (1968) calculated 1280 m for total subsidence but he did not envisage a deep crater (Fig. 3). The key here is to distinguish between rapid syn-eruptive subsidence – which occurs during the eruption because material is moved upwards in the diatreme due to explosions, possibly to the atmosphere, making space for the diatreme infill to subside – from post-eruptive subsidence, which results from slow compaction of the diatreme infill during diagenesis.

Post-eruptive subsidence is due to mechanical porosity reduction and chemical reactions (Suhr et al. 2006 and references therein). For the former process, the amount of initial pore space is limited in poorly sorted pyroclastic deposits typical of diatremes. So the scope for mechanical compaction seems limited (but has not been quantified). Alteration of juvenile particles to palagonite or clay probably reduces volume, but alteration of olivine crystals to serpentine causes a counterbalancing increase in volume (Suhr et al. 2006), so the role of chemical compaction is unclear. In any case, the available evidence from other localities is that post-eruptive subsidence may lower the top of the bedded infill of a deep diatreme by as much as a couple hundred of meters at the centre, at most 300 m (Suhr et al. 2006; Lorenz 2007).

So if post-eruptive subsidence only accounts for say 200 m, syn-eruptive subsidence must have dragged down the bedded pyroclastic material deposited on the crater floor, as well as the early-formed parts of the tephra ring and steeply dipping Wasatch Formation megablocks, by 0.8-1.1 km or more. This large calculated distance of syn-eruptive subsidence has to be explained, because it seems to represent an extreme end-member case in the spectrum of possibilities (White and Ross 2011). Syn-eruptive subsidence is caused by displacement of material from the deep part of the diatreme to or toward the surface, to make space for the subsiding beds.

Francis (1970) proposed that "cauldron" subsidence along ring faults in Scottish diatremes was due to "late-stage withdrawal of magma" occurring "shortly after eruption ended". However, it is not clear where the magma was stored, and where it then migrated to create space for the bedded pyroclastic rocks to subside into.

Lorenz (1975) shows a figure where in a mature diatreme, a central "eruption channel" sends pyroclastic debris upward from the base of the diatreme to the crater floor, and presumably to the atmosphere. This allows the existing diatreme infill, and the "collar of wall-rocks surrounding the vent", to subside during continuing phreatomagmatic activity. The material moving upward in the channel is "ejected, and deposited in part outside, in part outside the crater". Centroclinal bedding is due to "drag along the ring-fault" in this model.

Our explanation for syn-eruptive subsidence is similar to that of Lorenz (1975) in that in a mature diatreme, debris jets created by phreatomagmatic explosions in the deep diatreme or root zone send pyroclastic material upward (possibly to the crater floor, but not necessarily), and this creates space for the subsiding pyroclastic beds and sedimentary megablocks. The debris jets can occur in the centre of the diatreme in map view, but can also occupy other

positions laterally, depending on where the explosions are occurring. This explains the presence of more than one column of non-bedded pyroclastic material in some MRBVF diatremes. Lorenz and Kurszlaukis (2007) present the root zone as the only place where phreatomagmatic explosions occur and "feeder channels" originate, whereas White and Ross (2011) mention the possibility of "intra-diatreme fragmentation zones".

5.6 Emplacement model for the Missouri River Breaks diatremes

Bringing all our observations and interpretations together, we propose an emplacement model for the MRBVF diatremes. A cautionary note is that only a small part of the overall maar-diatreme volcanic system has been directly observed in the MRBVF, and the rest is inferred based on observations made in other volcanic fields. Specifically, the feeder dykes, root zones and lower parts of the diatremes are still hidden, whereas erosion has removed the maar craters and their post-eruptive infill, the surrounding tephra rings, and more than 1 km of upper diatreme rocks. Our emplacement model has four stages (Fig. 14): (a) propagation of the dyke, (b) formation of the proto-diatreme, (c) growth of the system and (d) post-eruptive events.

5.6.1 Propagation of the dyke

Mafic to ultramafic monogenetic volcanoes of all types are thought to originate from dykes rising from the mantle through pre-existing or new fractures/faults (Rubin 1995; Carrigan 2000; Lorenz 2000; Valentine and Gregg 2008). In the MRBVF, the ultramafic magma rose through a Precambrian basement, then through a succession of predominantly unconsolidated sedimentary formations comprising several aquifers at different depths (Fig. 14a).

5.6.2 Formation of a proto-diatreme

Phreatomagmatic explosions can occur at any depth less than about 2 km if aquifers are present (Valentine and White 2012). Nonetheless, phreatomagmatic fragmentation is more efficient at lower pressures, so explosions closer to the surface typically create the initial crater (Lorenz 1986, 2000, 2003, 2007; Büttner and Zimanowski 2003; Valentine et al. 2012; Valentine and White 2012) (Fig. 14a). At this initial stage, a deep diatreme is not expected.

Each shallow explosion sends fragmented magma and country rocks into the atmosphere in a water-rich eruptive column or jet. Deposits of pyroclastic density currents, fallback and fallout fill the syn-eruptive crater and become part of the proto-diatreme. A certain quantity of this pyroclastic material is deposited around the crater to form the tephra ring. During this initial stage, the proto-diatreme pyroclastic deposits are probably non-bedded (Ross et al. 2013) or bedding is destroyed by subsequent explosions since the initial crater and proto-diatreme are narrow and shallow. Later, the crater and diatreme will increase in width and depth and consequently many bedded deposits will be preserved (Fig. 14b).

5.6.3 Growth of the system

Explosions may continue to occur at different depths along the dike (Valentine and White 2012) but intra-diatreme fragmentation can also occur since the diatreme infill can be wholly or partly water-saturated (White and McClintock 2001; White and Ross 2011). At this stage, debris jets may not always reach the surface and will start to form columns of non-bedded pyroclastic material (Ross and White 2006; Ross et al. 2008a, 2008b) (Fig. 14b). The pyroclastic material expelled into the atmosphere, on the other hand, will continue to be deposited on the tephra ring and crater floor, where a bedded sequence will form and then be carried deeper into the diatreme due to syn-eruptive subsidence. Parts of the tephra ring may also collapse into the crater and then subside in the diatreme. Explosions within the diatreme or root zone can send material into the atmosphere (or move it to the shallow part of the diatreme), and the removal of material from depth creates a volume deficit, which allows syn-eruptive subsidence. Because the diatreme is cone-shaped, bedding in the pyroclastic deposits may not be preserved (or may never form) in the deep part. The syn-eruptive subsidence mechanism leads to the formation of megablocks of country rocks detaching from the shallow diatreme or crater walls. These will also sink with the enclosing pyroclastic deposits. Detachment of megablocks widens the crater and upper diatreme. Megablocks can be disintegrated by further explosions (White 1991; White and McClintock 2001), but some will be preserved. The upper part of the diatreme will widen more than the deepest part because phreatomagmatic fragmentation is less efficient and the rock more resistant at depth (Valentine and White 2012). Towards the end of the eruption, clastic dykes can form and coherent ultramafic dikes/plugs may be emplaced.

5.6.4 Post-eruptive events

Post-eruptive subsidence is envisaged to have occurred due to compaction of the diatreme fill during diagenesis. Over geological time, the MRBVF maar-diatreme volcanoes and enclosing country rocks were partly eroded.

5.7 Comparison with class 1 kimberlitic diatremes

There are many interesting similarities between class 1 kimberlitic diatremes (e.g., the classic kimberlite

pipes of South Africa; Clement and Reid 1989) and the MRBVF diatremes: (i) an ultramafic magma composition; (ii) a wide and deep diatreme with steep walls (Hawthorne 1975; Brown and Valentine 2013); (iii) the presence of non-vesicular spherical to sub-spherical juvenile pyroclasts, called pelletal lapilli in kimberlite pipes (Clement 1982; Mitchell 1986; Lloyd and Stoppa 2003; Brown et al. 2009); (iv) the abundance of lithic fragments (Kurszlaukis and Barnett 2003; Mitchell et al. 2009; Brown et al. 2009); (v) the occurrence of various amounts of bedded pyroclastic rocks (Lorenz 1975, 1986; Kurszlaukis and Barnett 2003; Sparks et al. 2006; Brown et al. 2008, 2009; Cas et al. 2008a, 2008b; Field et al. 2008); (vi) columns of non-bedded pyroclastic deposits (Clement 1982; Lorenz and Kurszlaukis 2007; Kurszlaukis and Lorenz 2008) and (vii) megablocks ("floating reefs") (Lorenz 1975; Lorenz and Kurszlaukis 2007; Field et al. 2008; Cas et al. 2009; Mitchell et al. 2009). This suggests that class 1 kimberlites and the MRBVF diatremes (and other maar-diatreme volcanoes) may have formed through similar mechanisms. Although phreatomagmatic models have been proposed for class 1 kimberlites (Lorenz 1975, 1985, 1986; Zimanowski et al. 1986; Lorenz et al. 1994; Lorenz and Kurszlaukis 1997; McClintock et al. 2009; White and Ross 2011), many authors prefer magmatic models (e.g., Sparks et al. 2006; Wilson and Head 2007; Cas et al. 2008a, 2008b; Mitchell et al. 2009; Gernon et al. 2012).

However, magmatic models fail to explain the abundance of lithic fragments in pyroclastic rocks, the significant proportion of ash, and the lack of vesicles in the juvenile products found in kimberlites; these features are typical of phreatomagmatic deposits. Moreover, the presence of well-bedded pyroclastic rocks in the MRBVF diatremes, and elsewhere, is incompatible with models calling upon a single and violent eruption (e.g., Sparks et al. 2006; Wilson and Head 2007; Cas et al. 2008b; Porritt and Cas 2009). Instead, multiple explosions are required to form the observed bedding (as also noted by Lorenz and Kurszlaukis 2007, Kurszlaukis and Lorenz 2008). The multiple explosions model is more consistent with volume fluxes (one m^3/s or less) at mafic monogenetic volcanoes. This means that small batches of magma that might accumulate over minutes or tens of minutes are the source of explosion energy (Valentine et al. 2011; Valentine and White 2012; Lefebvre et al. 2013).

6. Conclusions

In this paper we have considered five representative diatremes out of the >50 known in the Missouri River Breaks volcanic field (MRBVF). Their most striking feature is the dominance of bedded pyroclastic rocks at depths 1.3-1.5 km below the pre-eruptive surface. Bedded pyroclastic rocks accumulated on the crater floor as the eruption progressed and subsided large distances, mostly during the eruption; this makes these volcanoes an end-member case in the spectrum of diatreme infill possibilities. The other end-member cases, applicable to other volcanic fields, are diatremes containing few or no bedded pyroclastic rocks in their upper parts, and the "type II" bedded diatreme infills which accumulate subsequent to major excavation and are "effectively tuff rings, tuff cones or scoria cones that are initiated in open craters and accumulate to the fill the craters" (White and Ross 2011).

The studied MRBVF diatremes have a phreatomagmatic origin, as shown by the significant proportion of ash-sized particles, the lack of vesicles in the juvenile clasts, and the large proportions of lithic fragments in pyroclastic deposits. Further arguments supporting (but not proving) a phreatomagmatic origin are the inferred deposits of dilute pyroclastic currents within the diatremes and the presence of ash aggregates interpreted as accretionary and armored lapilli. Bedded pyroclastic rocks and non-bedded pyroclastic columns provide evidence for multiple explosions of variable intensity occurring at different depths and lateral positions in the diatreme. The presence of angular ash aggregates and accretionary lapilli in both bedded and non-bedded rocks indicates recycling of the pyroclastic material.

A first major conclusion from this study is that the soft-substrate did not influence the diatreme morphology: Wide, steep diatremes 1.3-1.5 km beneath the pre-eruptive surface do not conform to the general idea for the emplacement of diatremes in soft substrates. The diatremes were never deep open holes, otherwise the soft substrate would have collapsed. The second important conclusion is that subsidence played a major role during evolution of the diatremes, as highlighted by (i) shallow-sourced megablocks that travelled downward in the diatreme, (ii) concave-upward bedding of pyroclastic rocks in the diatreme, these beds having originally been deposited on the crater floor; and (iii) collars of downward-shifted country rocks around the diatremes. We calculate 1.0-1.3 km of total subsidence in the diatremes and estimate that 0.8 to 1.1 km of this was syn-eruptive subsidence.

Acknowledgements

This contribution is derived from the first author's PhD thesis at INRS. V. Lorenz, J. Stix and P. Francus are acknowledged for their input on the thesis. The study was funded by NSERC (Discovery grant to PSR) and an INRS start-up grant. We thank V. Lorenz, S. Kurszlaukis and J.D.L. White for discussions during the 2009 Missouri River Breaks field workshop as well as field assistant M. Villemure for her precious help. G.A. Valentine and J.D.L. White kindly commented on the

manuscript prior to submission. M. Ort and an anonymous reviewer provided helpful comments on the submitted manuscript.

References

Alvarado GE, Soto GJ, Salani FM, Ruiz P, Hurtado de Mendoza L (2011) The formation and evolution of Hule and Río Cuarto maars, Costa Rica. J Volcanol Geotherm Res 201:342–356

Auer A, Martin U, Németh K (2007) The Fekete-hegy (Balaton Highland Hungary) "soft-substrate" and "hard-substrate" maar volcanoes in an aligned volcanic complex-Implications for vent geometry, subsurface stratigraphy and the palaeoenvironmental setting. J Volcanol Geotherm Res 159:225–245

Aranda-Gómez JJ, Luhr JF (1996) Origin of the Joya Honda maar, San Luis Potosí, México. J Volcanol Geotherm Res 74:1–18

Arndt NT (2003) Komatiites, kimberlites, and boninites. J Geophys Res. doi:10.1029/2002JB002157.

Befus KS, Hanson RE, Lehman TM, Griffin WR (2008) Cretaceous basaltic phreatomagmatic volcanism in West Texas: maar complex at Peña Mountain, Big Bend National Park. J Volcanol Geotherm Res 173:245–264

Bertotto GW, Bjerg EA, Cingolani CA (2006) Hawaiian and Strombolian style monogenetic volcanism in the extra-Andean domain of central-west Argentina. J Volcanol Geotherm Res 158:430–444

Bowen GJ, Beerling DJ, Koch PL, Zachos JC, Quattlebaum T (2004) A humid climate state during the Palaeocene/Eocene thermal maximum. Nature 432:495–499

Brown RJ, Valentine GA (2013) Physical characteristics of kimberlite and basaltic intraplate volcanism and implications of a biased kimberlite record. Geol Soc Am Bull 125:1224–1238

Brown RJ, Gernon T, Stiefenhofer J, Field M (2008) Geological constraints on the eruption of the Jwaneng Centre kimberlite pipe, Botswana. J Volcanol Geotherm Res 174:195–208

Brown RJ, Tait M, Field M, Sparks RSJ (2009) Geology of a complex kimberlite pipe (K2 pipe, Venetia Mine, South Africa): insights into conduit processes during explosive ultrabasic eruptions. Bull Volcanol 71:95–112

Brown RJ, Manya S, Buisman I, Fontana G, Field M, Mac Niocaill C, Sparks RSJ, Stuart FM (2012a) Eruption of kimberlite magmas: physical volcanology, geomorphology and age of the youngest kimberlitic volcanoes known on earth (the Upper Pleistocene/Holocene Igwisi Hills volcanoes, Tanzania). Bull Volcanol 74:1621–1643.

Brown RJ, Bonadonna C, Durant AJ (2012b) A review of volcanic ash aggregation. Phys Chem Earth 45–46:65–78

Buchel G, Lorenz V (1993) Syn-and post-eruptive mechanism of the alaskan Ukinrek maars in 1977. In: Negendank JFW, Zolitschka B (eds) Paleolimnology of European Maar Lakes. pp 15-60

Büttner R, Zimanowski B (1998) Physics of thermohydraulic explosions. Phys Rev E 57:5726–5729

Büttner R, Zimanowski B (2003) Phreatomagmatic explosions in subaqueous volcanism. In: White JDL et al. (eds) Explosive subaqueous volcanism. Am Geophys U Geophys Monograph 140:51–60

Büttner R, Dellino P, Zimanowski B (1999) Identifying magma–water interaction from the surface features of ash particles. Nature 401:688–690

Büttner R, Dellino P, Raue H, Sonder I, Zimanowski B (2006) Stress-induced brittle fragmentation of magmatic melts: theory and experiments. J Geophys Res 111:B08204.

Calvari S, Tanner LH (2011) The Miocene Costa Giardini diatreme, Iblean Mountains, southern Italy: model for maar-diatreme formation on a submerged carbonate platform. Bull Volcanol 73:557–576

Carrasco-Núñez G, Ort MH, Romero C (2007) Evolution and hydrological conditions of a maar volcano (Atexcac crater, Eastern Mexico). J Volcanol Geotherm Res 159:179–197

Carrigan CR (2000) Plumbing systems. In: Sigurdsson H, Houghton B, McNutt S, Rymer H, Stix J (eds) Encyclopedia of volcanoes. Academic Press, San Diego, pp 219–235

Cas RAF, Wright JV (1987) Volcanic successions: modern and ancient. Allen and Unwin, London, 528 pp.

Cas RAF, Hayman P, Pittari A, Porritt L (2008a) Some major problems with existing models and terminology associated with kimberlite pipes from a volcanological perspective, and some suggestions. J Volcanol Geotherm Res 174:209–225

Cas RAF, Porrit L, Pittari A, Hayman P (2008b) A new approach to kimberlite facies terminology using a revised general approach to the nomenclature of all volcanic rocks and deposits: descriptive to genetic. J Volcanol Geotherm Res 174:226–240

Cas RAF, Porrit L, Pittari A, Hayman P (2009) A practical guide to terminology for kimberlite facies: a systematic progression from descriptive to genetic, including a pocket guide. Lithos 112:183–190

Cashman KV, Sturtevant B, Papale P, Navon O (2000) Magmatic fragmentation. In: Sigurdsson H, Houghton B, McNutt S, Rymer H, Stix J (eds) Encyclopedia of volcanoes. Academic Press, San Diego, pp 421–430

Chough SK, Sohn YK (1990) Depositional mechanics and sequences of base surges, Songaksan tuff ring, Cheju Island, Korea. Sedimentology 37:1115–1135

Christiansen RL, Foulger GR, Evans JR (2002) Upper-mantle origin of the Yellowstone hotspot. Geol Soc Am Bull 114:1245–1256

Cioni R, Marianelli P, Santagroce R, Sbrana A (2000) Plinian and subplinian eruptions. In: Sigurdsson H, Houghton B, McNutt S, Rymer H, Stix J (eds) Encyclopedia of volcanoes. Academic Press, San Diego, pp 477–494

Clement CR (1982) A comparative geological study of some major kimberlite pipes in the North Cape and Orange Free State. Unpublished Ph.D. dissertation, University of Cape Town, South Africa, 432 p.

Clement CR, Reid AM (1989) The origin of kimberlite pipes: an interpretation based on a synthesis of geological features displayed by southern African occurrences. In Ross et al. (eds.), Kimberlites and Related Rocks. Geol Soc Aus Sp Pub 14:632–646

Crowe BM, Fisher RV (1973) Sedimentary structures in base-surge deposits with special reference to cross-bedding,

Ubehebe craters, Death Valley, California. Geol Soc Am Bull 84:663–682
Delpit S (2013) From maar to diatremes: Pali Aike (Argentina) and Missouri River Breaks (United-States) volcanic fields. PhD thesis. Institut national de la recherche scientifique, Québec, Canada, 320 p
Dostal J, Breitsprecher K, Church BN, Thorkelson D, Hamilton TS (2003) Eocene melting of Precambrian lithospheric mantle: analcime-bearing volcanic rocks from the Challis-Kamloops belt of south central British Columbia. J Volcanol Geotherm Res 126:303–326
Downes PJ, Ferguson D Griffin BJ (2007) Volcanology of the Aries micaceous kimberlite, central Kimberley Basin, Western Australia. J Volcanol Geotherm Res 159:85–107
Downey JS, Dinwiddie GA (1988) The regional aquifer system underlying the Northern Great Plains in parts of Montana, North Dakota, South Dakota, and Wyoming - summary. Regional aquifer-system analysis. US Geol Surv Professional Paper 1402-A, 64 pp.
Dudás FÖ (1991) Geochemistry of igneous rocks from the Crazy Mountains, Montana, and tectonic models for the Montana alkalic province. J Geophys Res 96:13261–13277
Duke GI (2009) Black-Hills - Alberta carbonatite-kimberlite linear trend: Slab edge at depth? Tectonophysics 464:186–194
Field M, Stiefenhofer J, Robey J, Kurszlaukis S (2008) Kimberlite-hosted diamond deposits of southern Africa: a review. Ore Geol Rev 34:33–75
Fisher RV, Waters AC (1970) Base surge bed forms in maar volcanoes. Am J Sci 268:157–180
Fisher RV, Schmincke HU (1984) Pyroclastic Rocks. Springer-Verlag, Berlin, 472 pp.
Foreman BZ, Heller PL, Clementz T (2012) Fluvial response to abrupt global warming at the Palaeocene/Eocene boundary. Nature. doi:10.1038/nature11513
Francis EH (1970) Bedding in Scottish (Fifeshire) tuff-pipes and its relevance to maars and calderas. Bull Volcanol 34:697-712
Freda C, Gaeta M, Kamer DB, Marra F, Renne PR, Taddeucci J, Scarlato P, Christensen JN, Dallai L (2006) Eruptive history and petrologic evolution of the Albano multiple maar (Alban Hills, Central Italy). Bull Volcanol 68:567–591.
Gençalioglu-Kuscu G, Atilla C, Cas RAF, Kuşcu İ (2007) Base surge deposits, eruption history, and depositional processes of a wet phreatomagmatic volcano in Central Anatolia (Cora Maar). J Volcanol Geotherm Res 159:198–209
Gernon TM, Brown RJ, Tait MA, Hincks TK (2012) The origin of pelletal lapilli in explosive kimberlite eruptions. Nature Communications. doi:10.1038/ncomms1842
Gernon TM, Upton BGJ, Hincks TK (2013) Eruptive history of an alkali basaltic diatreme from Elie Ness, Fife, Scotland. Bull Volcanol 75:1-20
Geshi N, Németh K, Oikawa T (2011) Growth of phreatomagmatic explosion craters: a model inferred from Suoana crater in Miyakejima Volcano, Japan. J Volcanol Geotherm Res 201:30–38
Gilbert JS, Lane SJ (1994) The origin of accretionary lapilli. Bull Volcanol 56:398–411
Hawthorne JB (1975) Model of a kimberlite pipe. In: Ahrens LH, Dawson JB, Duncan AR, Erlank AJ (eds) Phys Chem Earth 9, Pergamon Press, pp 1–15
Hearn Jr BC (1968) Diatremes with kimberlitic affinities in north-central Montana. Science 159:622–625
Hearn Jr BC (1979) Preliminary map of diatremes and alkali ultramafic intrusions, Missouri River Breaks and vicinity, north-central Montana. U S Geol Surv, Open File Report 79-1128, scale 1:125,000
Hearn Jr BC (2009) Missouri Breaks diatremes: Field Trip July 2009. Field Trip Guidebook (informal), 35 pp.
Hearn Jr BC (2012) Missouri River Breaks diatremes, Montana, USA. Hopi Buttes volcanic field workshop. Abstract.
Hearn Jr BC, Swadley WC, Pecora WT (1964) Geology of the Rattlesnake quadrangle, Bearpaw Mountains, Blaine County, Montana. US Geol Surv, Bull 1181-B, 66 pp.
Hooten JA, Ort MH (2002) Peperite as a record of early-stage phreatomagmatic fragmentation processes: an example from the Hopi Buttes volcanic field, Navajo Nation, USA. J Volcanol Geotherm Res 114:95-106
Houghton B, Wilson CJN (1989) A vesicularity index for pyroclastic deposits. Bull Volcanol 51:451–462
Houghton BF, Smith RT (1993) Recycling of magmatic clasts during explosive eruptions: estimating the true juvenile content of phreatomagmatic volcanic deposits. Bull Volcanol 55:414–420
Houghton BF, Wilson CJM, Smith IEM (1999) Shallow-seated controls on styles of explosive basaltic volcanism: a case study from New Zealand. J Volcanol Geotherm Res 91:97–120, 44 pp
Irving AJ, Hearn Jr BC (2003) Alkalic rocks of Montana: kimberlites, lamproites, and related magmatic rocks. Guidebook prepared for the VIIIth International Kimberlite Conference, Montana Field Trip
Jordan SC, Cas RAF, Hayman PC (2013) The origin of a large (>3 km) maar volcano by coalescence of multiple shallow craters: Lake Purrumbete maar, southeastern Australia. J Volcanol Geotherm Res 254:5-22
Kienle J, Kyle PR, Self S, Motyka R, Lorenz V (1980) Ukinrek Maars, Alaska, I. Eruption sequence, petrology and tectonic setting. J Volcanol Geotherm Res 7:11–37.
Kurszlaukis S, Barnett WP (2003) Volcanological and structural aspects of the Venetia Kimberlite Cluster - a case study of South African kimberlite maar-diatreme volcanoes. S Afr J Geol 106:145–172
Kurszlaukis S, Lorenz V (2008) Formation of “Tuffisitic Kimberlites” by phreatomagmatic processes. J Volcanol Geotherm Res 174:68–80
Kwon CW, Sohn YK (2008) Tephra-filled volcanic neck (diatreme) of a mafic tuff ring at Maegok, Miocene Eoil Basin, SE Korea. Geosci J 12:317-329.
Lautze NC, Houghton BF (2007) Linking variable explosion style and magma textures during 2002 at Stromboli volcano, Italy. Bull Volcanol 69:445–460.
Kurszlaukis S, Buttner R, Zimanowski B, Lorenz V (1998) On the first experimental phreatomagmatic explosion of a kimberlite melt. J Volcanol Geotherm Res 80:323–326
Lefebvre NS, White JDL, Kjarsgaard BA (2013) Unbedded diatreme deposits reveal maar-diatreme-forming eruptive processes: Standing Rocks West, Hopi Buttes, Navajo Nation, USA. Bull Volcanol 75:739.

Lloyd E, Stoppa F (2003) Pelletal lapilli in diatremes - some inspiration from the Old Masters. GeoLines 15:65–71
Lorenz V (1973) On the formation of maars. Bull Volcanol 37:183–203
Lorenz V (1975) Formation of phreatomagmatic maar-diatreme volcanoes and its relevance to kimberlite diatremes. Phys Chem Earth 9, Pergamon Press, pp 17–27
Lorenz V (1985) Maars and diatremes of phreatomagmatic origin: a review. Trans Geol Soc S Afr 88:459–470
Lorenz V (1986) On the growth of maars and diatremes and its relevance to the formation of tuff rings. Bull Volcanol 48:265–274
Lorenz V (2000) Formation of maar-diatreme volcanoes. Terra Nostra 2000/6. International Maar Conference, Daun/Vulkaneifel, p. 284–291
Lorenz V (2003) Maar-diatreme volcanoes, their formation, and their setting in hard-rock or soft-rock environments. GeoLines 15:72–83
Lorenz V (2007) Syn- and posteruptive hazards of maar-diatreme volcanoes. J Volcanol Geotherm Res 159:285–312
Lorenz V, Kurszlaukis S (1997) On the last explosions of carbonatite pipe G3b, Gross Brukkaros, Namibia. Bull Volcanol 59:1–9
Lorenz V, Kurszlaukis S (2007) Root zone processes in the phreatomagmatic pipe emplacement model and consequences for the evolution of maar-diatreme volcanoes. J Volcanol Geotherm Res 159:4–32
Lorenz V, Zimanowski B, Fröhlich G (1994) Experiments on explosive basic and ultrabasic, ultramafic, and carbonatitic volcanism. Proc 5th Int Kimb Conf, Araxa Brazil, CPRM Spec Publ 1:270–284
Lorenz V, Zimanowski B, Büttner R (2002) On the formation of deep-seated subterranean peperite-like magma–sediment mixtures. J Volcanol Geotherm Res 114:107–118
Macdonald R, Upton BGJ, Collerson KD, Hearn Jr BC, James D (1992) Potassic mafic lavas of the Bearpaw Mountains, Montana: mineralogy, chemistry, and origin. J Petrol 33:305–346
Martín-Serrano A, Vegas J, García-Cortés A, Galán L, Gallardo-Millán JL, Martín-Alfageme S, Rubio FM, Ibarra PI, Granda A, Pérez-González A, García-Lobón JL (2009) Morphotectonic setting of maar lakes in the Campo de Calatrava Volcanic Field (Central Spain, SW Europe). Sedim Geol 222:52–63
McCallum ME (1976) An emplacement model to explain contrasting mineral assemblages in adjacent kimberlite pipes. J Geol 84:673–684
McClintock M, White JDL (2006) Large phreatomagmatic vent complex at Coombs Hills, Antarctica: wet, explosive initiation of flood basalt volcanism in the Ferrar-Karoo LIP. Bull Volcanol 68:215–239
McClintock M, Ross PS, White JDL (2009) The importance of the transport system in shaping the growth and form of kimberlite volcanoes. Lithos 112S:465–472
Miller JA, Appel CL (1997) Ground water atlas of the United States. US Geol Surv, 300 pp.
Mirnejad H, Bell K (2006) Origin and source evolution of the Leucite Hills lamproites: evidence from Sr-Nd-Pb-O isotopic compositions. J Petrol 47:2463–2489
Mitchell RH (1986) Kimberlites: Mineralogy, Geochemistry and Petrology. Plenum Press, New York. 442 pp.
Mitchell RH, Skinner EMW, Scott Smith BH (2009) Tuffisitic kimberlites from the Wesselton Mine, South Africa: mineralogical characteristics relevant to their formation. Lithos 112S:452–464
Moore JG (1967) Base surge in recent volcanic eruptions. Bull Volcanol 30:337–363
Moore JG, Kasuaki N, Alcaraz A (1966) The 1965 eruption of Taal volcano. Science 151:955–960
Morrissey MM, Mastin LG (2000) Vulcanian eruptions. In: Sigurdsson H, Houghton B, McNutt S, Rymer H, Stix J (eds) Encyclopedia of volcanoes. Academic Press, San Diego, pp 463–475
Naidoo P, Stiefenhofer J, Field M, Dobbe R (2004) Recent advances in the geology of Koffiefontein Mine, Free State, South Africa. Lithos 76:161–182
Németh K, Martin U (2007) Shallow sill and dyke complex in western Hungary as a possible feeding system of phreatomagmatic volcanoes in "soft-rock" environment. J Volcanol Geotherm Res 159:138–152
Németh K, Martin U, Harangi Sz (2001) Miocene phreatomagmatic volcanism at Tihany (Pannonian Basin, Hungary). J Volcanol Geotherm Res 111:111–135
Németh K, Martin U, Haller MJ, Alric VI (2007) Cenozoic diatreme field in Chubut (Argentina) as evidence of phreatomagmatic volcanism accompanied with extensive Patagonian plateau basalt volcanism. Episodes, J Int Geosci 30:217–223
Németh K, Haller MJ, Martin U, Risso C, Massaferro G (2008) Morphology of lava tumuli from Mendoza (Argentina), Patagonia (Argentina), and Al-Haruj (Libya). Zeits für Geomorph 52:181–194
Németh K, Cronin SJ, Haller MJ, Brenna M, Csillag G (2010) Modern analogues for Miocene to Pleistocene alkali basaltic phreatomagmatic fields in the Pannonian Basin: "soft-substrate" to "combined" aquifer controlled phreatomagmatism in intraplate volcanic fields. Cent Eur J Geosciences 2:339–361
Ngwa Suh CE, Devey CW (2010) Phreatomagmatic deposits and stratigraphic reconstruction at Debunscha Maar (Mt Cameroon volcano). J Volcanol Geotherm Res 192:201-211
Nowicki T, Crawford B, Dyck D, Carlson J, McElroy R, Oshust P, Helmstaedt H (2004) The geology of kimberlite pipes of the Ekati property NWT, Canada. Lithos 76:1–27
O'Brien HE, Irving AJ, McCallum IS (1991) Eocene potassic magmatism in the Highwood Mountains, Montana: petrology, geochemistry, and tectonic implications. J Geophys Res 96:13237–13260
O'Brien HE, Irving AJ, McCallum IS, Thirlwall MF (1995) Strontium, neodymium, and lead isotopic evidence for the interaction of post-subduction asthenospheric potassic mafic magmas of the Highwood Mountains, Montana, USA, with ancient Wyoming craton lithospheric mantle. Geochem Cosmo Acta 59:4539–4556
Ort MH, Carrasco-Núñez G (2009) Lateral vent migration during phreatomagmatic and magmatic eruptions at Tecuitlapa Maar, east-central Mexico. J Volcanol Geotherm Res 181:67-77

Pardo N, Macias JL, Giordano G, Cianfarra P, Avellán DJ, Bellatreccia F (2009) The ~1245 yr BP Asososca maar eruption: The youngest event along the Nejapa–Miraflores volcanic fault, Western Managua, Nicaragua. J Volcanol Geotherm Res 184:292–312

Pirrung M, Büchel G, Jacoby W (2001) The Tertiary volcanic basins of Eckfeld, Enspel and Messel (Germany). Zeit Deut Geol Ges 152:27–59

Pioli L, Erlund E, Johnson E, Cashman K, Wallace P, Rosi M, Delgado Granados H (2008) Explosive dynamics of violent Strombolian eruptions: The eruption of Parícutin Volcano 1943-1952 (Mexico). Earth Planet Sci Lett 271:359–368

Porritt LA, Cas RAF (2009) Reconstruction of a kimberlite eruption, using an integrated volcanological, geochemical and numerical approach: a case study of the Fox Kimberlite, NWT, Canada. J Volcanol Geotherm Res 179:241–264

Porter KW, Wilde EM (2001) Geologic map of the Zortman 30' x 60' quadrangle, central Montana. Montana Bureau of Mines and Geology Open File Report MBMG 438.

Pyle DM (2000) Sizes of volcanic eruptions. In: Sigurdsson H, Houghton B, McNutt S, Rymer H, Stix J (eds) Encyclopedia of volcanoes. Academic Press, San Diego, pp 263–269

Raue H (2004) A new model for the fracture energy budget of phreatomagmatic explosions. J Volcanol Geotherm Res 129:99–108

Ross PS, White JDL (2006) Debris jets in continental phreatomagmatic volcanoes: A field study of their subterranean deposits in the Coombs Hills vent complex, Antarctica. J Volcanol Geotherm Res 149:62–84

Ross PS, White JDL (2012) Quantification of vesicle characteristics in some diatreme-filling deposits, and the explosivity levels of magma–water interactions within diatremes. J Volcanol Geotherm Res 245–246:55–67

Ross PS, White JDL, Zimanowski B, Büttner R (2008a) Rapid injection of particles and gas into non-fluidized granular material, and some volcanological implications. Bull Volcanol 70:1151–1168

Ross PS, White JDL, Zimanowski B, Büttner R (2008b) Multiphase flow above explosion sites in debris-filled volcanic vents: Insights from analogue experiments. J Volcanol Geotherm Res 178:104–112

Ross PS, Delpit S, Haller MJ, Németh K, Corbella H (2011) Influence of the substrate on maar-diatreme volcanoes - An example of a mixed setting from the Pali Aike volcanic field, Argentina. J Volcanol Geotherm Res 201:253–271

Ross PS, White JDL, Valentine GA, Taddeucci J, Sonder I, Andrews RG (2013) Experimental birth of a maar-diatreme volcano. J Volcanol Geotherm Res 260:1–12

Rubin AM (1995) Propagation of magma-filled cracks. Annu Rev Earth Planet Sci 23:287–336

Schipper CI, White JDL, Zimanowski B, Büttner R, Sonder I, Schmid A (2011) Experimental interaction of magma and "dirty" coolants. Earth Planet Sci Lett 303:323–336

Schumacher R, Schmincke HU (1991) Internal structure and occurrence of accretionary lapilli - a case study at Laacher See Volcano. Bull Volcanol 53:612–634

Schumacher R, Schmincke HU (1995) Models for the origin of accretionary lapilli. Bull Volcanol 56:626–639

Self S, Kienle J, Huot JP (1980) Ukinrek Maars, Alaska II. Deposits and formation of the 1977 craters. J Volcanol Geotherm Res 7:39–65

Son MS, Kim JS, Jung S, Ki JS, Kim MC, Sohn YK (2012) Tectonically controlled vent migration during maar–diatreme formation: An example from a Miocene half-graben basin in SE Korea. J Volcanol Geotherm Res 223–224:29–46

Sottili G, Taddeucci J, Palladino DM, Gaeta M, Scarlato P, Ventura G (2009) Sub-surface dynamics and eruptive styles of maars in the Colli Albani Volcanic District, Central Italy. J Volcanol Geotherm Res 180:189–202

Sottili G, Palladino DM, Gaeta M, Masotta M (2012) Origins and energetics of maar volcanoes: examples from the ultrapotassic Sabatini Volcanic District (Roman Province, Central Italy). Bull Volcanol 74:163–186.

Sparks RSJ, Baker L, Brown RJ, Field M, Schumacher J, Stripp G, Walters A (2006) Dynamical constraints on kimberlite volcanism. J Volcanol Geotherm Res 155:18–48

Stiefenhofer J, Farrow D (2004) Crater deposits of the Mwadui kimberlite. Lithos 76:139-160

Suhr P, Goth K, Lorenz V, Suhr S (2006) Long lasting subsidence and deformation in and above maar-diatreme volcanoes – a never ending story. Zeit Deut Ges Geow 157:491–511

Swenson FA, Durum WH (1955) Geology and ground-water resources of the Missouri River Valley in Northeastern Montana. US Geol Surv Water-supply Paper 1263, 128 pp

Taddeucci J, Valentine GA, Sonder I, White JDL, Ross P-S, Scarlato P (2013) The effect of pre-existing craters on the initial development of explosive volcanic eruptions: an experimental investigation. Geophys Res Lett 40:507-510

Valentine GA (2012) Shallow plumbing systems for small-volume basaltic volcanoes, 2: evidence from crustal xenoliths at scoria cones and maars. J Volcanol Geotherm Res 223–224:47–63

Valentine GA, Fisher RV (2000) Pyroclastic surges and blasts. In: Sigurdsson H, Houghton B, McNutt S, Rymer H, Stix J (eds) Encyclopedia of volcanoes. Academic Press, San Diego, pp 571–580

Valentine GA, Gregg TKP (2008) Continental basaltic volcanoes - processes and problems. J Volcanol Geotherm Res 177:857–873

Valentine GA, White JDL (2012) Revised conceptual model for maar-diatremes: subsurface processes, energetics, and eruptive products. Geology, 40:1111-1114

Valentine GA, Shufelt NL, Hintz ARL (2011) Models of maar volcanoes, Lunar Crater (Nevada, USA). Bull Volcanol 73:753–765

Valentine GA, White JDL, Ross PS, Amin J, Taddeucci J, Sonder I, Johnson PJ (2012) Experimental craters formed by single and multiple buried explosions and implications for volcanic craters with emphasis on maars. Geophys Res Lett. 39:Art. L20301

Van Eaton AR, Wilson CJN (2013) The nature, origins and distribution of ash aggregates in a large-scale wet eruption deposit: Oruanui, New Zealand. J Volcanol Geotherm Res 250:129–154

Vazquez JA, Ort MH (2006) Facies variation of eruption units produced by the passage of single pyroclastic surge currents, Hopi Buttes volcanic field, USA. J Volcanol Geotherm Res 154:222-236
Vergniolle S, Mangan M (2000) Hawaiian and strombolian eruptions. In: Sigurdsson H, Houghton B, McNutt S, Rymer H, Stix J (eds) Encyclopedia of volcanoes. Academic Press, San Diego, pp 447–461
Vespermann D, Schmincke HU (2000) Scoria cones and tuff rings. In: Sigurdsson H, Houghton B, McNutt S, Rymer H, Stix J (eds) Encyclopedia of volcanoes. Academic Press, San Diego, pp 683–694
Waters AC, Fisher RV (1971) Base surges and their deposits: Capelinhos and Taal volcanoes. J Geophys Res 76:5596–5614
White JDL (1991) Maar-diatreme phreatomagmatism at Hopi Buttes, Navajo Nation (Arizona), USA. Bull Volcanol 53:239–258
White JDL (1996) Impure coolants and interaction dynamics of phreatomagmatic eruptions. J Volcanol Geotherm Res 74:155–170
White JDL, McClintock M (2001) Immense vent complex marks flood-basalt eruption in a wet, failed rift: Coombs Hills, Antarctica. Geology 29:935–938
White JDL, Houghton BF (2006) Primary volcaniclastic rocks. Geology 34:677–680
White JDL, Ross PS (2011) Maar-diatreme volcanoes: a review. J Volcanol Geotherm Res 201:1–29
Wilde EM, Porter KW (2001) Geologic map of the Winifred 30' x 60' quadrangle, central Montana. Montana Bureau of Mines and Geology Open File 437, scale 1:100,000
Wilson L, Head JW (2007) An integrated model of kimberlite ascent and eruption. Nature 447:53–57
Wohletz K, Sheridan MF (1983) Hydrovolcanic explosions. II. Evolution of basaltic tuff rings and tuff cones. Am J Sci 283:385–413
Zimanowski B (1998) Phreatomagmatic explosions. In: Freundt A, Rosi M (eds) From magma to tephra: modeling physical processes of explosive volcanic eruptions. Elsevier 25–53
Zimanowski B, Lorenz V, Frohlich G (1986) Experiments on phreatomagmatic explosions with silicate and carbonatitic melts. J Volcanol Geotherm Res 30:149–153
Zimanowski B, Büttner R, Lorenz V, Häfele H-G (1997) Fragmentation of basaltic melt in the course of explosive volcanism. J Geophys Res 102:803–814
Zimanowski B, Wohletz KH, Büttner R, Dellino P (2003) The volcanic ash problem. J Volcanol Geotherm Res 122:1–5

Figures

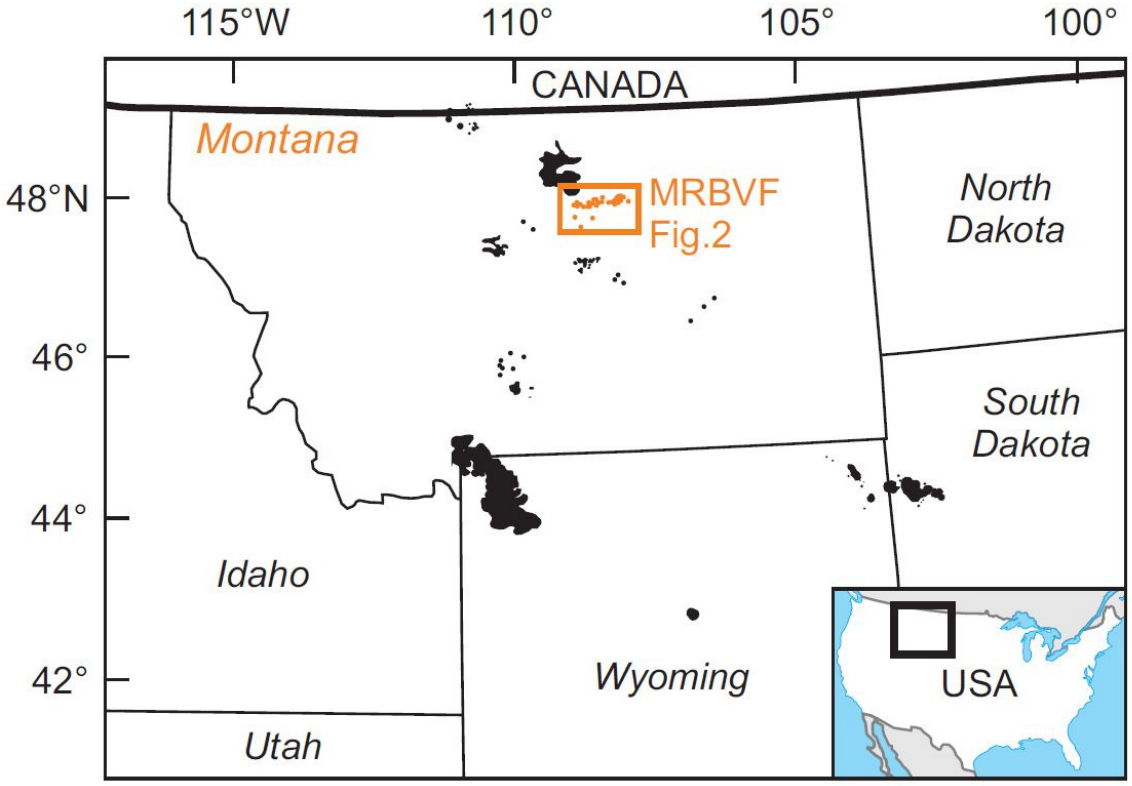

Figure 1. Location of the Paleocene-Eocene Great Plains alkalic province and the Missouri River Breaks volcanic field. Igneous centers from the alkalic province are represented by black and orange areas. Modified from Duke (2009).

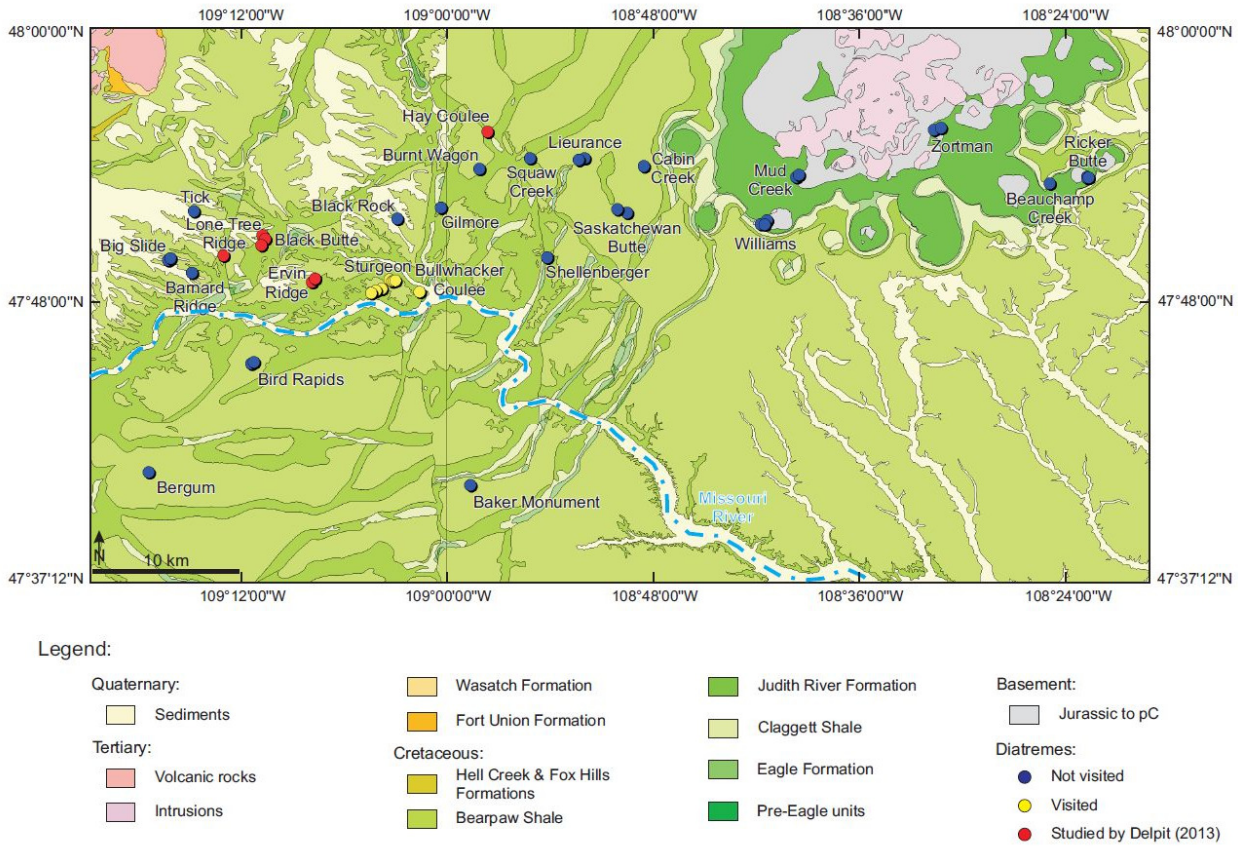

Figure 2. Geological map and location of the MRBVF diatremes. Four diatremes were studied in detail by Delpit (2013) (red spots). In addition, the Bullwhacker Coulee diatreme and a few others were visited (yellow spots). These diatremes were emplaced through a >2 km-thick succession of Upper Cretaceous to lower Eocene predominantly unconsolidated sedimentary formations and middle Eocene clastic deposits from the Bearpaw Mountains volcanic field (Hearn 1968, 1979, 2012).

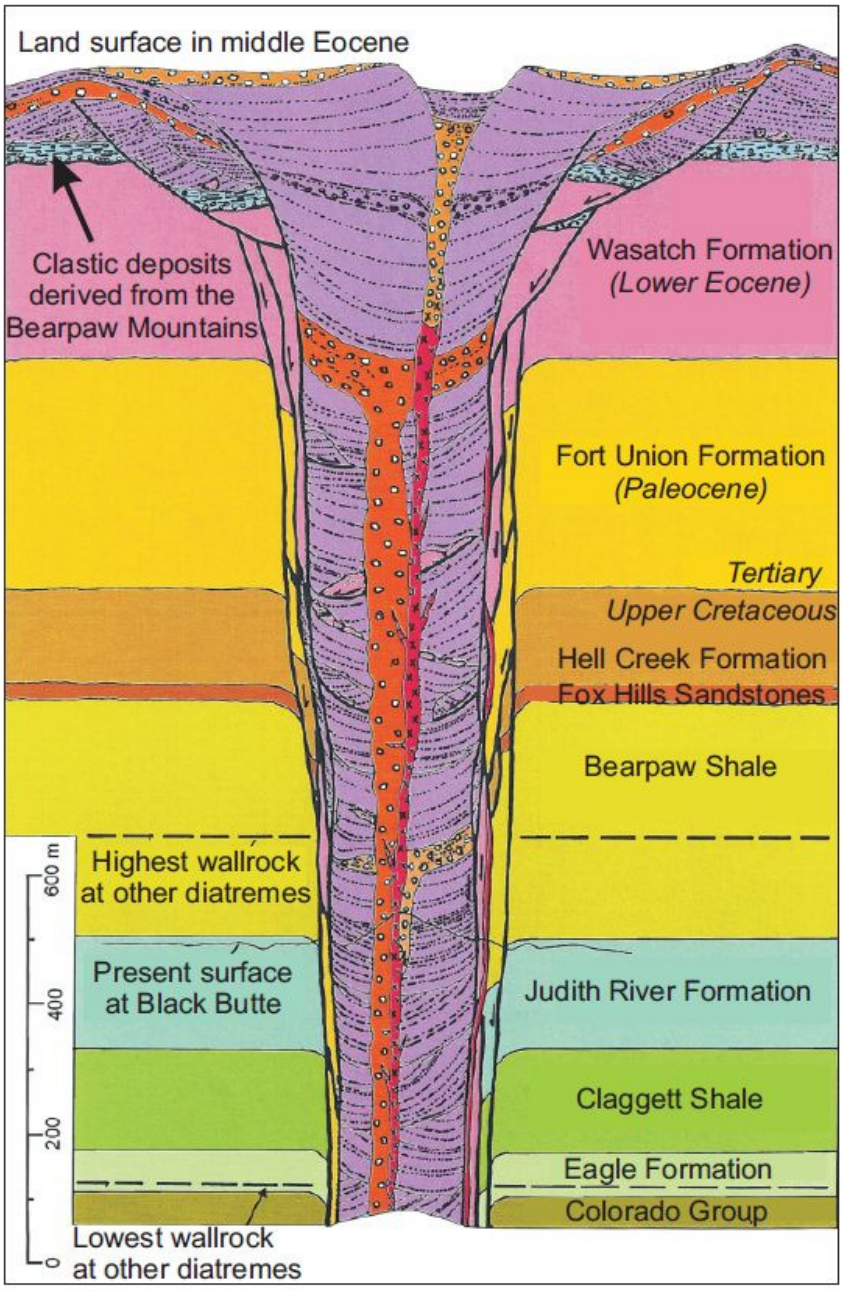

Figure 3. Stratigraphic cross-section of the sedimentary formations of the MRBVF area and schematic reconstruction of a diatreme (after Hearn 1968). Thickness of the sedimentary formations have been measured in the Bearpaw Mountains area.

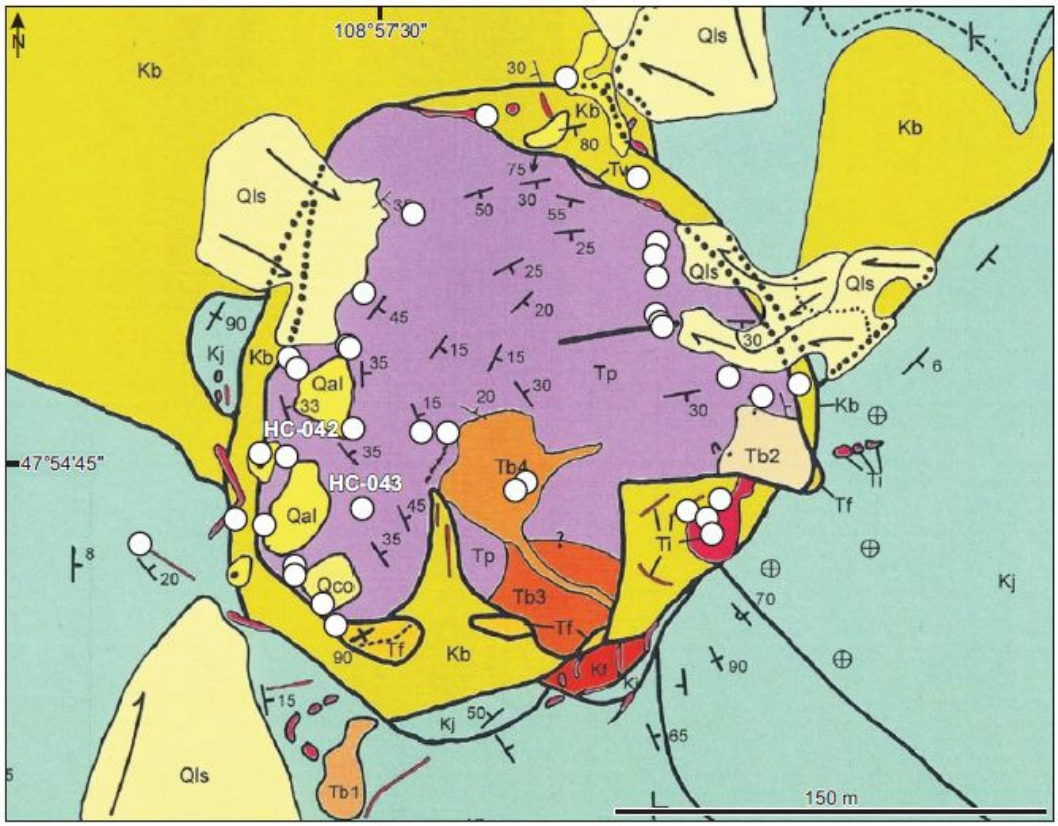

Qal Alluvium

Qco Colluvium: rockfall of large blocks of Judith River Formation

Qls Landslide deposits of Bearpaw Shale and Judith River Formation

} Quaternary

Ti Intrusive igneous rocks

Tb4 Coarse non-bedded lapilli tuff rich in sub-spherical to spherical juvenile pyroclasts, up to block size, and in sedimentary blocks

Tb3 Non-bedded pyroclastic deposits with blocks of siltstone and coal derived from the Fort Union Formation

Tb2 Coarse non-bedded lapilli tuff with blocks of sandstone and abundant juvenile material

} Middle Eocene

Tb1 Non-bedded pyroclastic deposits with sedimentary fragments, igneous rocks and abundant blocks of Cretaceous sandstone and shale

Tp Bedded pyroclastic deposits. Beige to greenish

} Middle Eocene

Tw Wasatch Formation } Lower Eocene

Tf Fort Union Formation (short dashes = traceable bed) } Paleocene

Kf Fox Hills Sandstone; area includes some sandy beds of uppermost Bearpaw Shale

Kb Bearpaw Shale

Kj Judith River Formation (short dashes = traceable bed)

} Upper Cretaceous

Figure 4. Geological map of Hay Coulee diatreme. Each observation and/or sampling station is symbolized by a white circle. Map from Hearn (2009), legend after Hearn (2009) and new field observations (Delpit 2013).

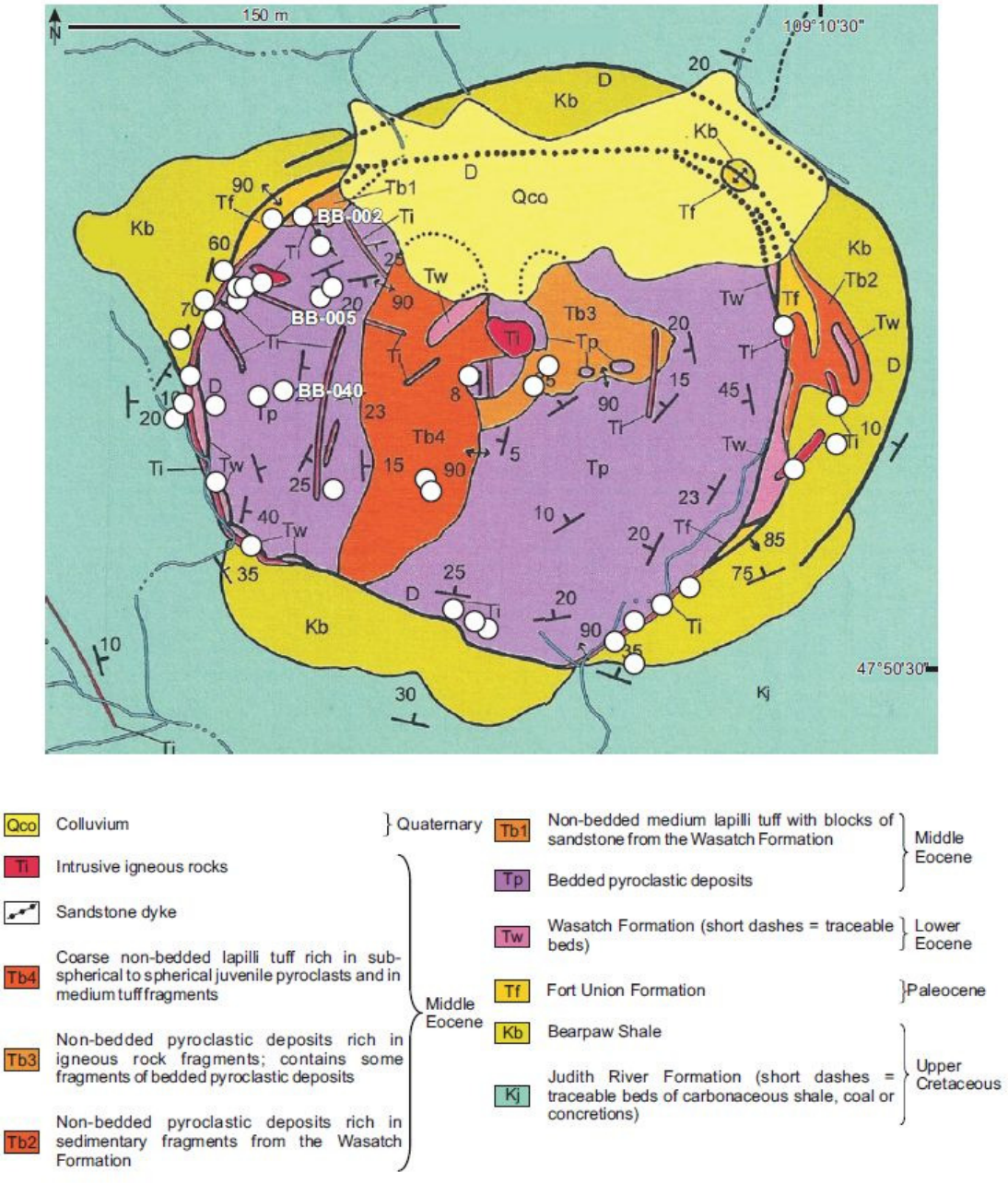

Figure 5. Geological map of Black Butte diatreme. Each observation and/or sampling station is symbolized by a white circle. Map from Hearn (2009), legend after Hearn (2009) and new field observations (Delpit 2013).

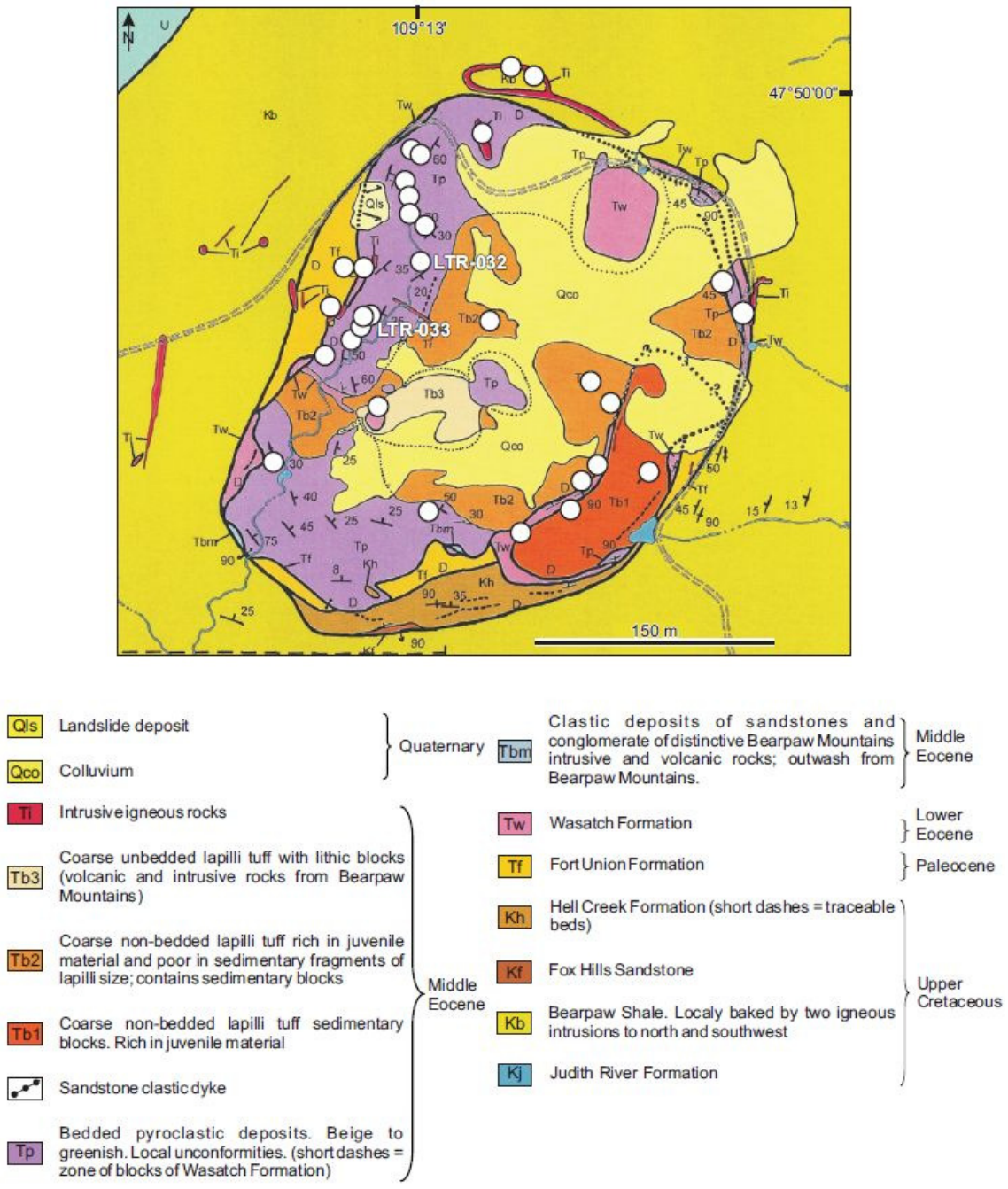

Figure 6. Geological map of Lone Tree Ridge diatreme. Each observation and/or sampling station is symbolized by a white circle. Map from Hearn (2009), legend after Hearn (2009) and new field observations (Delpit 2013).

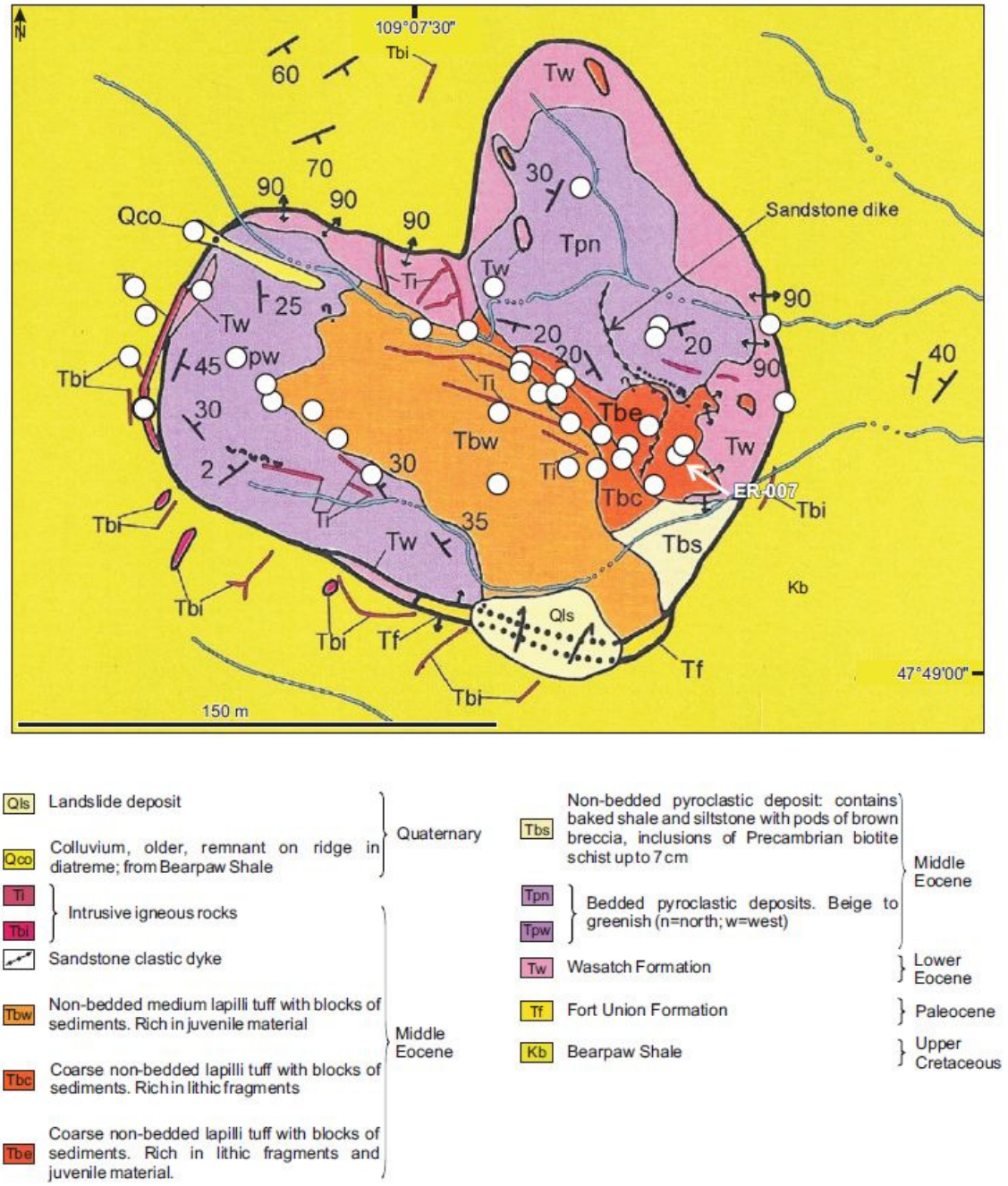

Figure 7. Geological map of Ervin Ridge diatreme. Each observation and/or sampling station is symbolized by a white circle. Map from Hearn (2009), legend after Hearn (2009) and new field observations (Delpit 2013).

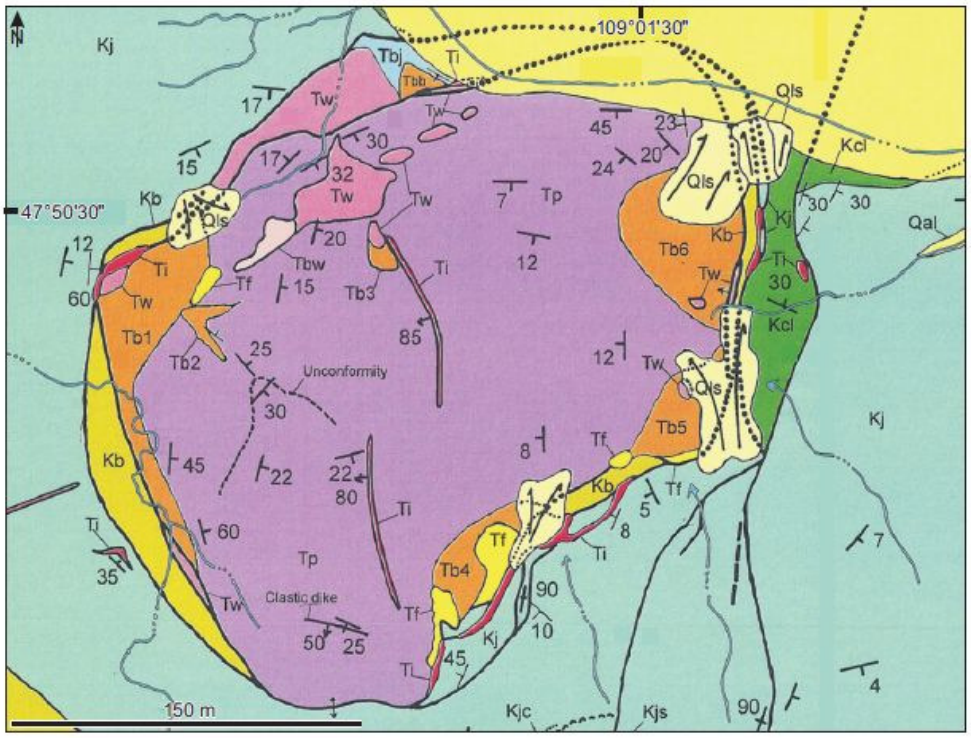

Qal Alluvium
Qls Landslide deposits
} Quaternary

Ti Intrusive igneous rock or igneous breccia dyke

Tb6 Non-bedded pyroclastic material with coarse, massive, igneous rock fragments + blocks of baked shale and bedded pyroclastic deposits up to 1 m size + spherical to subspherical juvenile pyroclasts

Tb5 Non-bedded pyroclastic material with igneous rock fragments + sparse limestone fragments and crustal metamorphic rock fragments

Tb4 Non-bedded pyroclastic material with massive, igneous rock fragments + 30% baked shale, siltstone, and sandstone

Tb3 Non-bedded pyroclastic material with igneous rock fragments, up to 0.3 m size

Tb2 Non-bedded pyroclastic material with green, igneous rock fragments + spherical to subspherical juvenile pyroclasts

} Middle Eocene

Tb1 Non-bedded pyroclastic material with massive, igneous rock fragments + sedimentary rock fragments

Tbw Non-bedded pyroclastic material with Wasatch Formation fragments + bedded pyroclastic deposits fragments

Tbj Non-bedded pyroclastic material with Judith River Formation material

Tbb Non-bedded pyroclastic material with Bearpaw Shale fragments + Cretaceous sandstone fragments + igneous rock fragments

Tp Bedded pyroclastic deposits

} Middle Eocene

Tw Wasatch Formation — } Lower Eocene

Tf Fort Union Formation — } Paleocene

Kb Bearpaw Shale

Kj Judith River Formation

Kcl Claggett Shale

} Upper Cretaceous

Figure 8. Geological map of Bullwhacker Coulee diatreme. Map from Hearn (2009), legend after Hearn (2009) and new field observations (Delpit 2013).

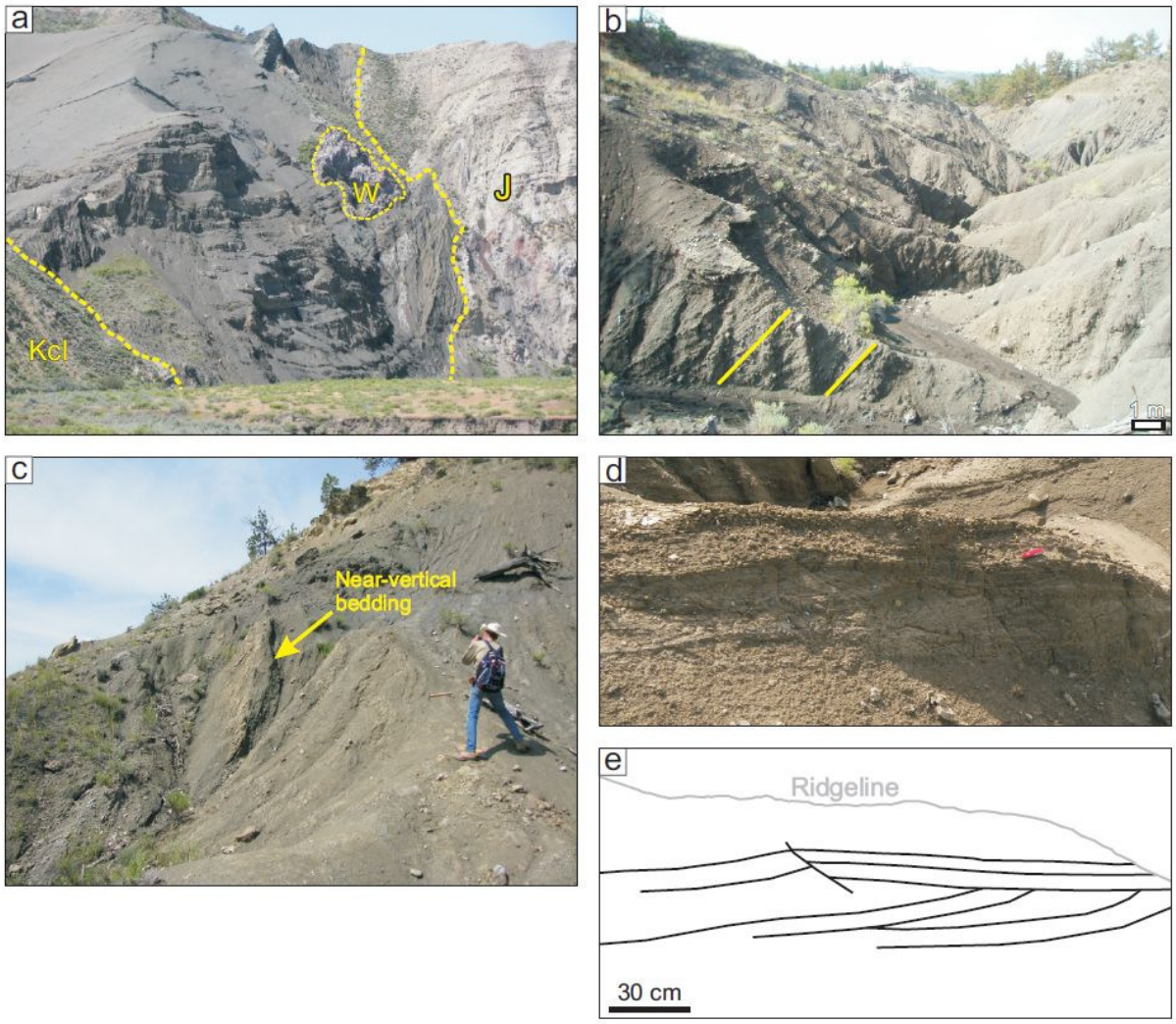

Figure 9. Bedded pyroclastic rocks. (a) At Bullwhacker Coulee diatreme, pyroclastic beds dominate the infill and dip toward the center of the diatreme, with steeper angles along the walls. Host rocks are mostly Upper Cretaceous Judith River Formation (J) and bend downward near the diatreme. Claggett Shale (Kcl) was uplifted here in and along the fault striking ~N10E. A 35-m-long megablock from the lower Eocene Wasatch Formation (W) sits in the diatreme, at least 1 km down from its source. (b)-(c) Bedded pyroclastic rocks at Lone Tree Ridge diatreme. Beds are steep near the diatreme margins (b) becoming near-vertical at the contact with the country rocks (c). (d)-(e) Photo and line drawing of low-angle trough-shaped cross-bedding within pyroclastic rocks at Lone Tree Ridge diatreme (photo courtesy of J.D.L. White).

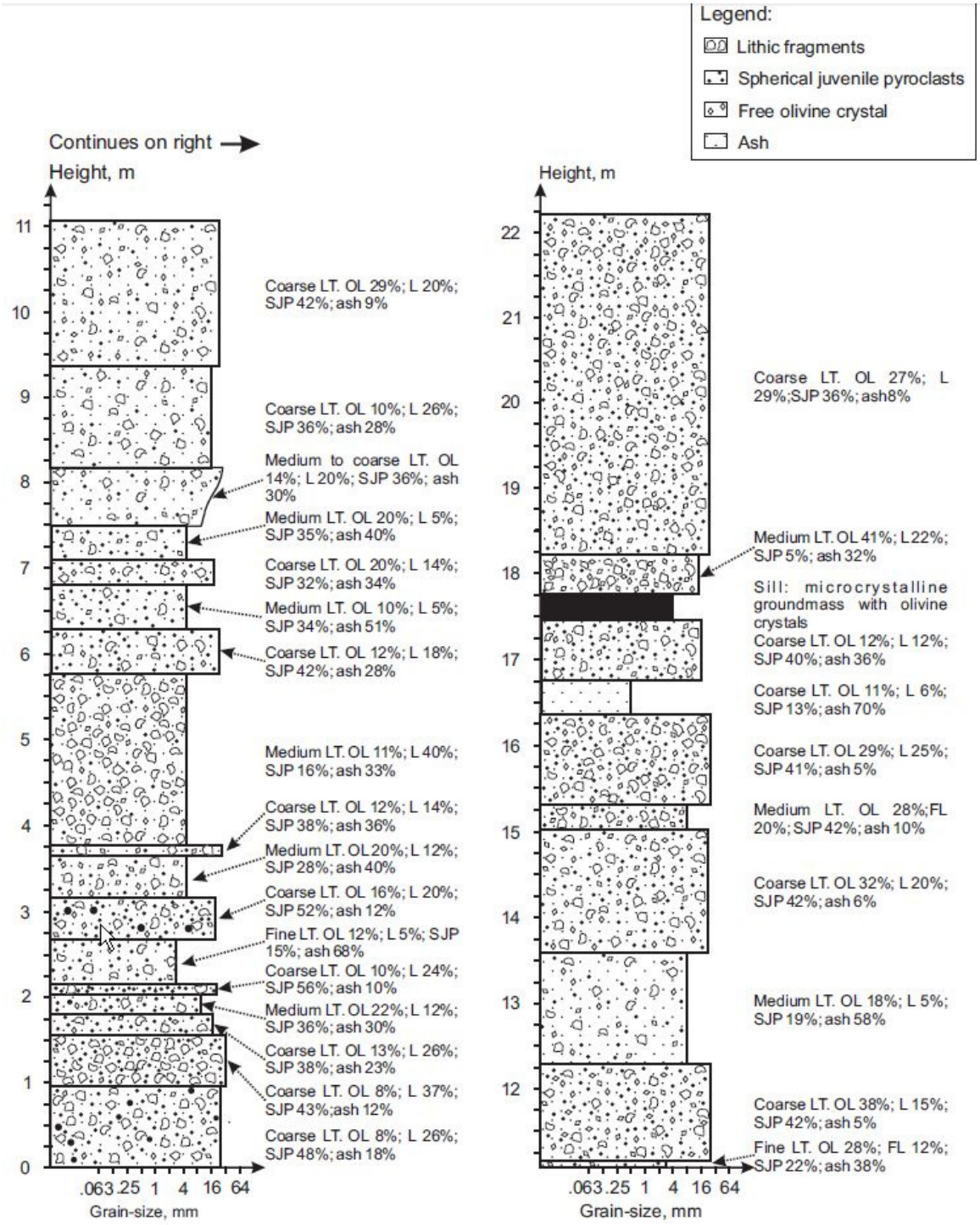

Figure 10. Graphic log of bedded pyroclastic rocks at station BB-040 in the Black Butte diatreme (see Fig. 5 for location). LT = lapilli tuff; OL = Olivine; L = lithic; SJP = Spherical juvenile pyroclast.

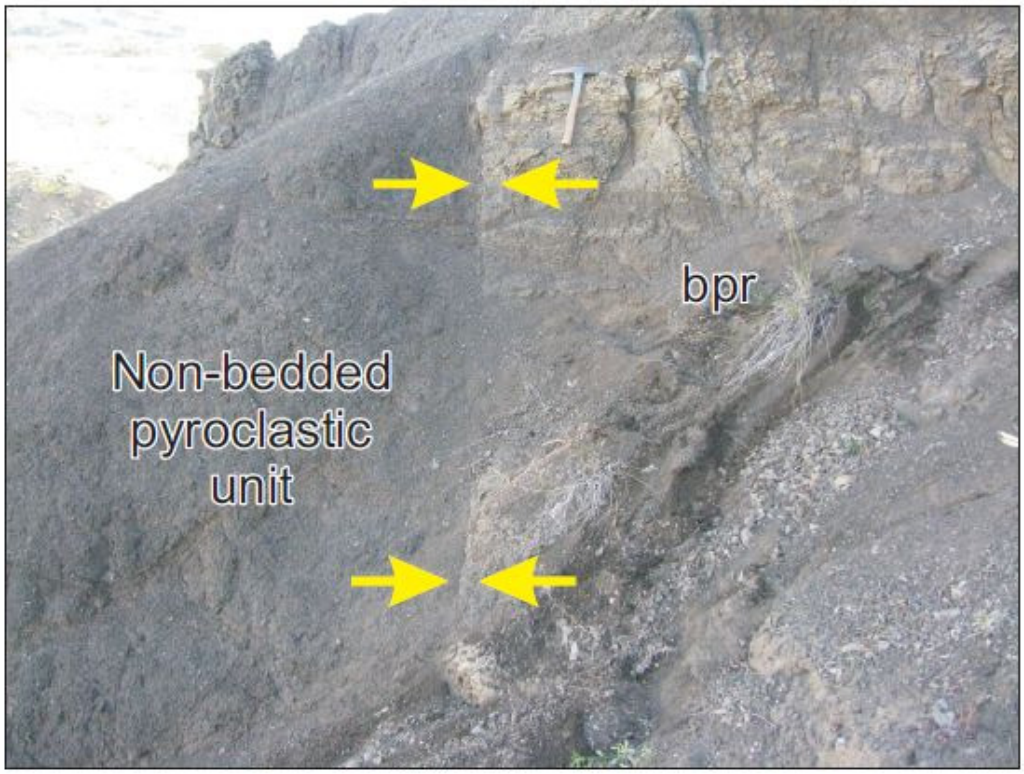

Figure 11. Non-bedded pyroclastic rocks at Black Butte diatreme, cutting across bedded pyroclastic rocks (bpr). The contact is sharp, near-vertical, and passes between the arrows. Hammer for scale.

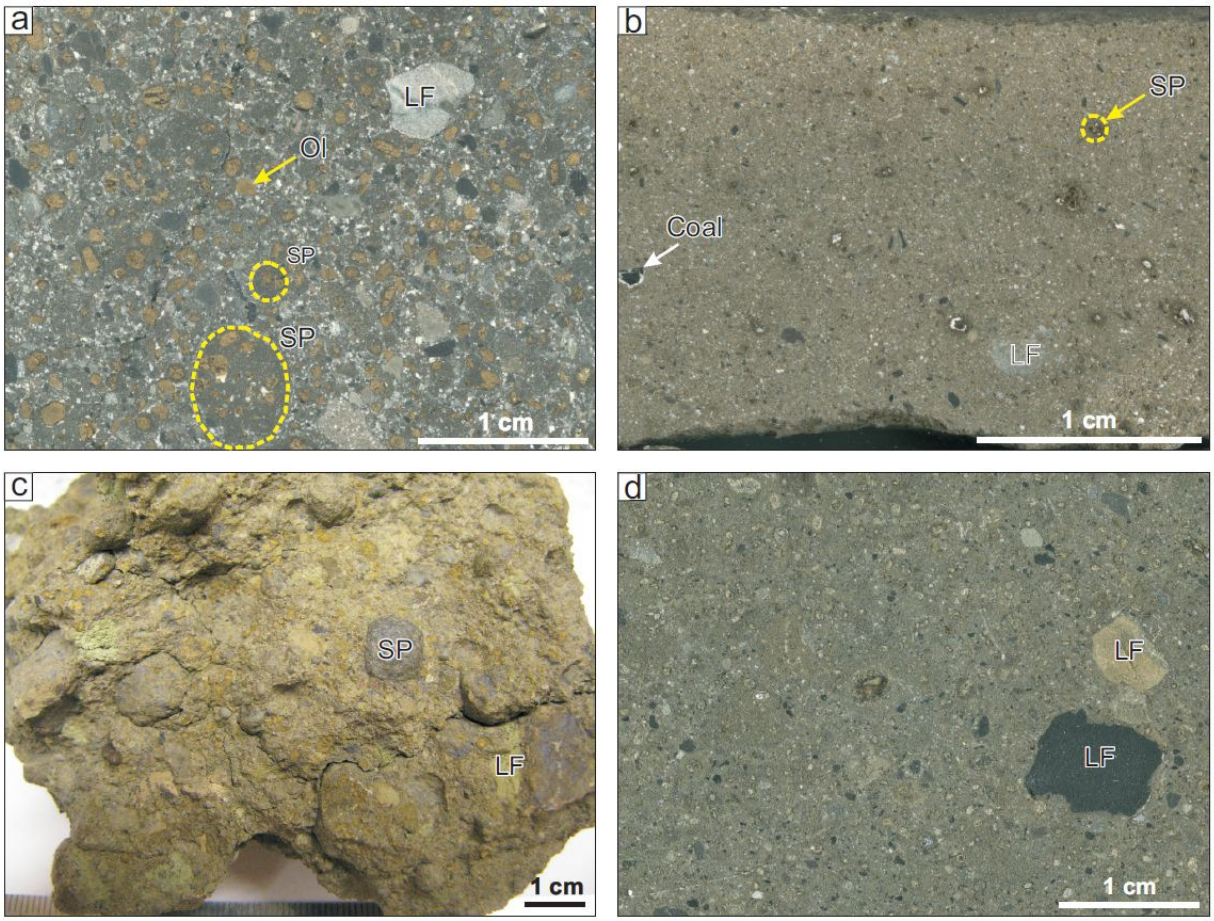

Figure 12. Components and textures of pyroclastic rocks. (a) Coarse lapilli tuff sampled at the BB-040 station in Black Butte diatreme. This sample is very rich in spherical to sub-spherical juvenile pyroclasts (SP) but contains some sedimentary lithic fragments (LF) and very few free altered olivine crystals (Ol). (b) Very coarse tuff sampled at the HC-042 station in Hay Coulee diatreme. This sample is rich in sedimentary lithic fragments and contains a few spherical to sub-spherical juvenile pyroclasts. (c) Lithic-rich medium lapilli tuff sampled at the BB-002 station in Black Butte diatreme. This sample contains a large proportion of sedimentary lithics and a few spherical to sub-spherical juvenile pyroclasts. (d) Lithic-bearing coarse lapilli tuff sampled at the ER-007 station in Ervin Ridge diatreme. The photos are from slabs except (c), which is a hand sample.

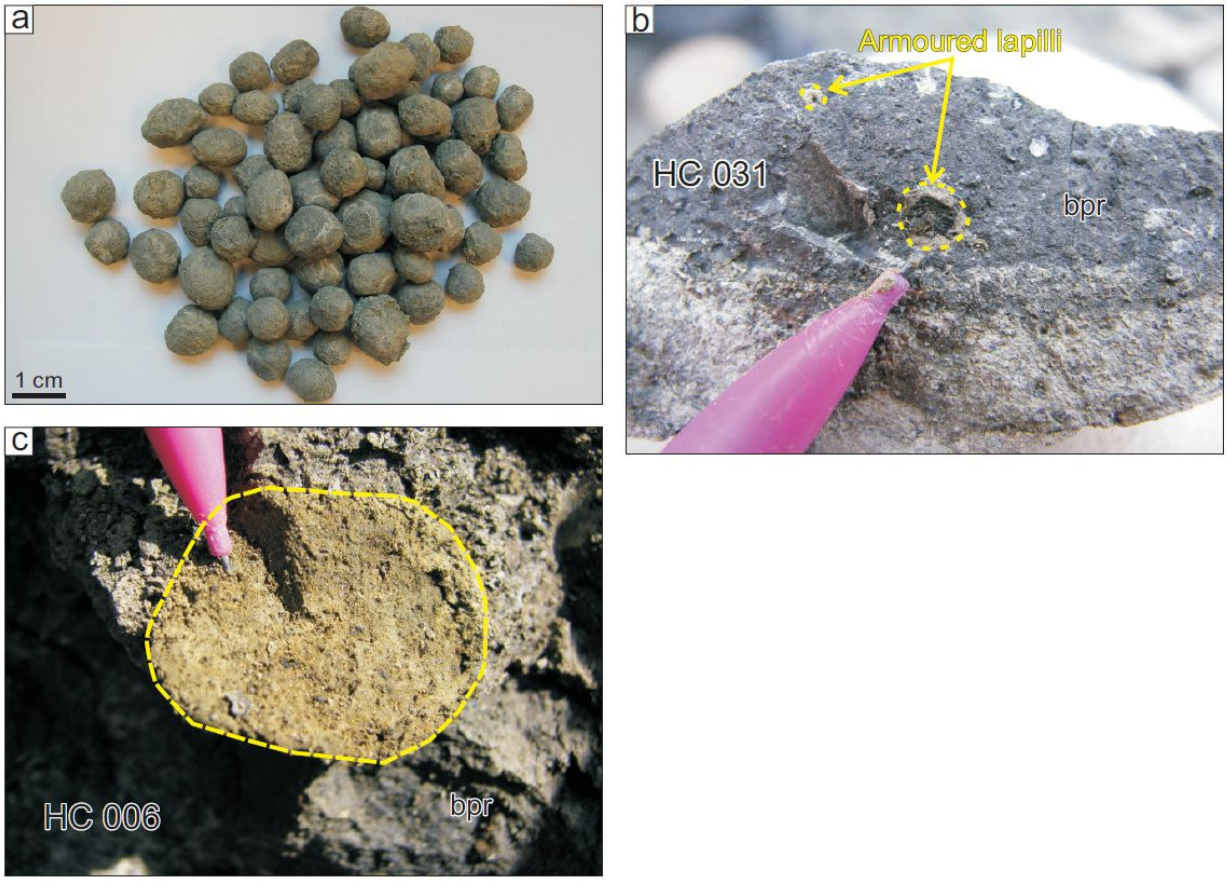

Figure 13. Spherical to sub-spherical juvenile pyroclasts and ash aggregates. (a) A collection of 1 cm-wide spherical to sub-spherical juvenile pyroclasts extracted from pyroclastic rocks at the Hay Coulee diatreme. (b) Armoured lapilli composed of altered olivine crystals surrounded by fine ash. The sample is derived from a bedded pyroclastic rock (bpr) at the HC-031 station in Hay Coulee diatreme. (c) Ash aggregate of spherical shape from the HC-006 station in bedded pyroclastic rocks (bpr) at Hay Coulee diatreme.

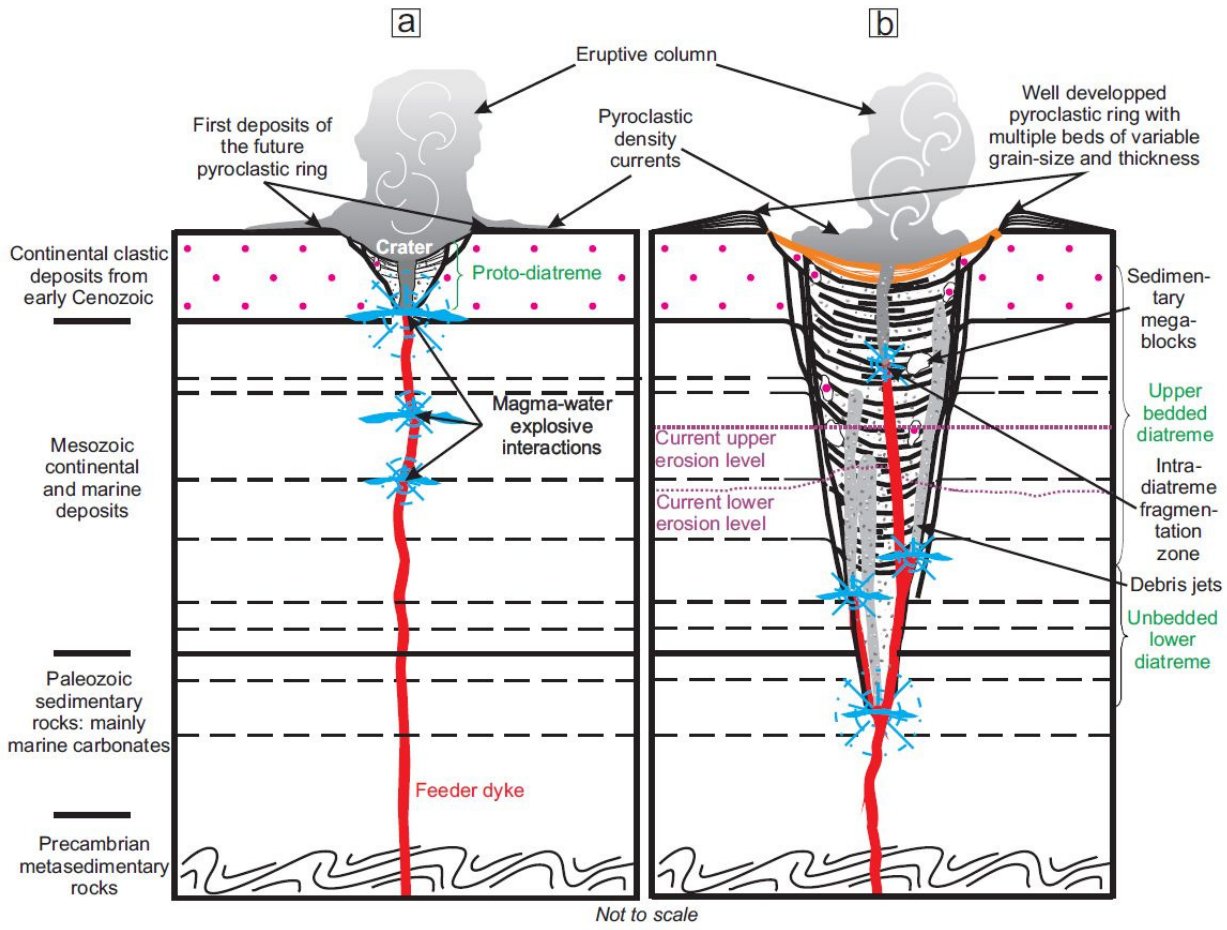

Figure 14. Emplacement model for the MRBVF maar-diatreme volcanoes. (a) The magma rises through the sedimentary substrate, which is mainly unconsolidated in the first kilometers under the surface. It encounters one or several aquifers (represented in blue) at different depths and interacts explosively, leading to fragmentation of the magma and the surrounding country rocks. The fragmented material from the shallowest explosions is erupted into the atmosphere, forming an eruptive column, and a crater is formed. At this stage, a proto-diatreme is developing. (b) Towards the end of the eruption, the diatreme is of conical shape with a well developed pyroclastic ring surrounding the maar crater that cuts the pre-eruptive surface. The upper diatreme is bedded whereas the lower diatreme is not. As a response to syn-eruptive subsidence, the bedded pyroclastic material develops a bowl-shaped structure; megablocks of younger age are now at deeper levels in the diatreme and layers of the country rock record a downward movement along the diatreme walls. Debris jets form at any level within the diatreme as a result of phreatomagmatic explosions and their non-bedded deposits cut pre-existing pyroclastic deposits. Currently, depending of the diatreme, the erosion level is in the Bearpaw Shale or Judith River Formation. The black dashed lines represent schematically the bedding within the sedimentary sequence.